Journal of Marine Research, 48, 591–639, 1990

A nitrogen-based model of plankton dynamics in the oceanic mixed layer

by M. J. R. Fasham,[1] H. W. Ducklow[2] and S. M. McKelvie[2]

ABSTRACT

As a first step toward the development of coupled, basin scale models of ocean circulation and biogeochemical cycling, we present a model of the annual cycles of plankton dynamics and nitrogen cycling in the oceanic mixed layer. The model is easily modified and runs in FORTRAN on a personal computer. In our initial development and exploration of the model's behavior we have concentrated on modeling the annual cycle at Station "S" near Bermuda using seven compartments (Phytoplankton, Zooplankton, Bacteria, Nitrate, Ammonium, Dissolved organic nitrogen and Detritus). This choice of compartments and the attendant flows (fluxes or intercompartmental exchanges) permits a functional distinction between new and regenerated production. We have examined over 200 different runs and carried out sensitivity analyses. Results of model runs with detrital sinking rates of 1 and 10 meters per day are presented. In these runs, the phytoplankton biomass-specific mortality rate was varied to adjust the annual net primary production (NPP) for the mixed layer to a value equivalent to 45 gC m^{-2}, which was calculated from the literature. Modelled cycles of zooplankton and bacterial stocks, and magnitudes of their annual production which cannot be validated due to sparse observations, are driven by the amplitude of the spring bloom and by changes in foodweb structure. Most, but not all model runs exhibit a spring bloom triggered by the winter depression of zooplankton stocks and the vernal increase in solar irradiance. The bloom is driven by nitrate entrained into the mixed layer during the wintertime deepening of the mixed layer. Following the shoaling of the pycnocline to ca 20 m, nitrate supply is limited to diffusional inputs, nitrate stocks are depleted, and regenerated production exceeds new production. The resulting cycles of new and regenerated production produce an annual cycle of the *f*-ratio with winter maxima approaching 0.8–0.9 and summer minima reaching ca 0.1–0.2, with annual values averaging 0.7. The model reproduces the "Eppley Curve," a hyperbolic relationship of increasing *f* with increasing primary production. This curve is shown to be the trajectory of the production system in the *f*-NPP phase plane. These model runs reproduce the annual cycles of areal NPP, and average annual NPP, new production, and particulate N flux values reported in the literature. The model demonstrates that currently accepted values for these annual fluxes can be reconciled only if the *f*-ratio has a high annual average. At present, the annual average *f*-ratio is poorly quantified due to severe undersampling in fall and winter. Our model's ecological structure has been successfully incorporated into the Princeton general circulation model for the North Atlantic Ocean.

1. Institute of Oceanographic Sciences, Deacon Laboratory, Natural Environmental Research Council, Brook Road, Wormley, Godalming, United Kingdom, GU8 5UB.

2. Horn Point Environmental Laboratories, University of Maryland, Center for Environmental and Estuarine Sciences, P. O. Box 775, Cambridge, Maryland, 21613 U.S.A.

The behavior of the 7-compartment model at high latitudes and at the equator, and the properties of 9-compartment models with two size classes of phytoplankton and grazers, are now being examined.

1. Introduction

In the past decade, several developments have transformed biological oceanography. Results from the Coastal Zone Color Scanner (CZCS) have demonstrated great variability in phytoplankton biomass on local to global scales (Esaias *et al.*, 1986). New observational and measurement techniques have demonstrated the importance of microbial plankton in contributing to the productivity reflected in the CZCS images (Williams, 1981; Azam *et al.*, 1983; Ducklow, 1983). Eppley and Peterson (1979) hypothesized that oceanic new production (the fraction of primary production supported by externally-supplied nutrients) is equivalent over some large scale to the export of organic matter from the euphotic zone. This concept helps to unify the views of oceanic biology supplied by the satellite and the microscope, by suggesting mechanisms through which nutrient uptake by microbial plankton is related to large scale patterns of biogeochemical cycling. Both the satellite data and microbiological results have suggested the great importance of specifying seasonal cycles of plankton, nutrients and physical processes for a better understanding of ecosystem dynamics.

To date there have been few attempts to model the nutrient and plankton dynamics of the upper ocean in a way that includes the important microbial processes and nitrogen fluxes and contributes to large scale views of seasonal plankton cycles. Early models tended to concentrate on the interaction of phytoplankton and zooplankton only. More recently, models have become more holistic by attempting to embrace the totality of our knowledge of the components of the ecosystem and the flows of materials between these components (Pace *et al.*, 1984; Fasham, 1985; Moloney *et al.*, 1986; Parsons and Kessler, 1987). Williams (1981) provided the conceptual background for a plankton dynamics model incorporating bacteria, protozoans, and dissolved organic matter. Later Pace *et al.* (1984) presented results from a full simulation model incorporating a large number of groups of organisms and flows. The Pace *et al.* model included physical forcing parameterized in the form of variable nutrient inputs, but no explicit physical processes, nor a seasonal approach to the dynamics. Evans and Parslow (1985) provided the latter components in a simple model of phytoplankton-zooplankton-nitrogen dynamics in a seasonally varying mixed layer. They showed how the seasonal recurrence of plankton cycles, in particular the spring bloom, is driven by the interaction of physical mixing with removal by grazers. We have built on these developments to construct a simple but realistic model of plankton and nutrient dynamics of the oceanic mixed layer that includes the major plankton groups (phytoplankton, zooplankton, bacteria) and the major forms of nitrogen (new and recycled inorganic forms, dissolved and particulate organic forms). This model provides a tool for testing different hypotheses about foodweb structure and plankton dynamics, which

has facilitated the design of sub-models for integrated, basin-scale models of ocean circulation and biogeochemistry (Sarmiento *et al.*, 1990). Our overall objective is to use this approach to model the seasonal cycles of plankton and nutrients in the global ocean, in order to learn more about the role of oceanic biology in regulating the atmospheric CO_2 content.

In the following sections, we provide first a technical description of the model structure and function, then present the results of our attempts to arrive at a simulation of the cycles of plankton and nutrients off Bermuda. An analysis of the ecosystem seasonal dynamics is presented in some detail and, finally, the implications of the model results for the interpretation of observations of *f*-ratio and new production are discussed.

2. The model structure and equations

a. The model structure. Compartmental ecosystem models of the mixed layer have been widely used in marine ecology, beginning with the pioneering work of Steele (1958). They make the basic assumption that the mixed layer can be considered biologically homogeneous, which is equivalent to assuming that the physical mixing rate is fast compared to the growth rates of the organisms. This assumption is probably robust in most cases but may break down in areas, such as the northeast Atlantic, that have very deep mixed layers in the winter (Robinson *et al.*, 1979). We decided at the outset to design a software package that was generalized and modular and had the following capabilities:

1) The compartments, flows between compartments, and equations governing those flows would be defined at run-time and would not require program changes. This was achieved by building on the general ecosystem equations developed by Wiegert (1979).

2) Previous models often focused mainly on the state-variable concentrations to the exclusion of flows, whereas it is the flows that are critically important, both in understanding a model and in validating it with data (Platt *et al.*, 1981). The software was therefore designed so that intercompartmental flows, averaged over any specified time period, could be easily calculated.

3) Ecosystem seasonality was assumed to be driven by seasonal changes in incident photosynthetically active radiation (PAR) and mixed layer depth (Evans and Parslow, 1985).

Nitrogen is generally regarded as the limiting nutrient of primary production, an ability to model the seasonal nitrogen cycle is an essential prerequisite for understanding the carbon cycle. The use of nitrogen as a model currency has the additional advantage that the primary production can be partitioned into "new" production, fuelled by nitrate, and "regenerated" production, fuelled mainly by ammonium (Dugdale and Goering, 1967; Eppley and Peterson, 1979). This partitioning can be measured directly by ^{15}N uptake techniques and such data provide extra constraints on any model.

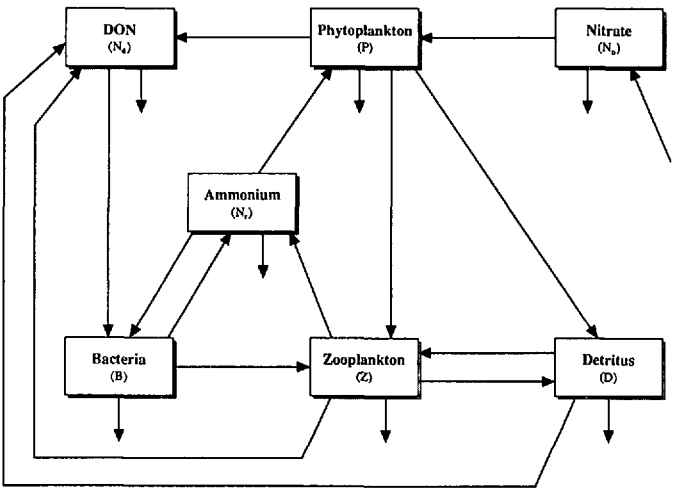

Figure 1. Diagrammatic representation of a nitrogen-based model of mixed layer plankton and nitrogen cycling showing the compartments and the modelled nitrogen flows among compartments and between compartments and the deep ocean.

We consider that the simplest model capable of capturing the essence of nitrogen cycling in the mixed layer requires seven compartments (Fig. 1). These compartments (with their mathematical symbols in parentheses) are:

1. Phytoplankton (P),
2. Zooplankton (Z),
3. Bacteria (B),
4. Nitrate nitrogen (N_n),
5. Ammonium nitrogen (N_r),
6. Labile dissolved organic nitrogen (N_d), and,
7. Detritus (D).

There has been much discussion recently on the role of dissolved organic matter (DOM) in the ocean (Toggweiler *et al.*, 1987; Williams and Druffel, 1988; Toggweiler, 1989) and the significance of bacteria in the breakdown and recycling of this material (Azam *et al.*, 1983; Ducklow, 1983). DON is comprised of a large number of poorly identified organic molecules only some of which are easily utilizable by bacteria (usually referred to as the labile fraction). The recent results of Sugimura and Suzuki (1988) show that a large amount of the DOM in the ocean is broken down very slowly and may form an important component in the remineralization cycle in the deep ocean. However, until this complex issue is more fully resolved we have decided to model only the labile fraction of DON that is rapidly utilized (with a time scale of order days) by bacteria.

The ammonium pool should also be understood to include other forms of regenerated

nitrogen, principally urea. In this simplified model, we have not specified a separate behavior for urea, though there is support for such a formulation, as current evidence suggests that bacteria cannot use it as a growth substrate (Wheeler and Kirchman, 1986; Goldman *et al.*, 1987). If this is true, then a more realistic model would have a separate urea compartment, with utilization by phytoplankton only. This would be analogous to the DON, which is taken up only by bacteria. Such a formulation would greatly increase the complexity of the model dynamics, and, for now has not been included.

The detritus compartment was defined as comprising fecal materials, and dead phytoplankton and zooplankton. It was assumed that detritus can be recycled within the mixed layer by two mechanisms, reingestion by zooplankton (Paffenhofer and Knowles, 1979; Poulet, 1983) or breakdown into DON and subsequent uptake by bacteria. In reality the latter process may be mediated by bacteria (Newell and Linley, 1984) attached to the surface of the detritus, and some models (e.g. Pace *et al.*, 1984) have included a separate compartment for attached bacteria. We consider this to be an unnecessary complication, especially bearing in mind the technical problems in distinguishing attached from free bacteria (Clarke and Joint, 1986). Detrital sinking is modelled by specifying a simple sinking rate and the resulting flux is considered to be exported from the mixed layer. This is a gross simplification as in reality detritus consists of a range of particles of differing origin, size, and sinking rates and so it is difficult, if not impossible, to assign one overall sinking rate to this melange of particles. We approached this problem by investigating the sensitivity of the simulations to different sinking rates. The detritus in our model is labile, with turnover times on the order of tens of days, and should not be confused with the total particulate organic nitrogen (PON) measured by CHN analyzers.

The state-variable units used are mMol Nitrogen m^{-3}. However, flows, such as primary production or particulate export from the mixed layer, are usually specified in areal units of mMol N m^{-2} per day, or per year.

b. Mixed layer depth equation. Following Evans and Parslow (1985) we have not attempted to model the mixed layer dynamics explicitly, but instead assume that data are available to define the seasonal change in mixed layer depth, M, as a function of time, t (days). Mathematically this can be written,

$$\frac{dM}{dt} = h(t) \tag{1}$$

Evans and Parslow (1985) pointed out that the effect of the deepening or shallowing of the mixed layer on the concentration of a state-variable will depend on whether that variable describes a nonmotile biotic, or abiotic, entity such as phytoplankton or detritus, or whether it describes a motile biotic entity like zooplankton. In the latter

case it might be assumed that the zooplankton are able actively to maintain themselves within the mixed layer when its depth changes, and so the volumetric concentration of zooplankton will decrease and increase when the mixed layer depth increases and decreases, respectively. However, in the case of nonmotile entities a deepening of the mixed layer will dilute the volumetric concentration, whereas when the mixed layer shallows, material is left behind, or detrained, but the volumetric concentration in the mixed layer will remain unchanged. Evans and Parslow (1985) dealt with this asymmetry by defining the variable, $h^+(t) = \max(h(t), 0)$, and using $h^+(t)$, rather than $h(t)$, in equations representing nonmotile entities.

c. Phytoplankton equation. The equation for phytoplankton can now be written as,

$$\frac{dP}{dt} = (1 - \gamma_1)\sigma(t, M, N_n, N_r)\, P - G_1 - \mu_1 P - \frac{(m + h^+(t))\, P}{M} \tag{2}$$

where $\sigma(t, M, N_n, N_r)$ is the average daily phytoplankton specific growth rate, G_1 represents the loss of phytoplankton due to zooplankton grazing, μ_1 is the specific natural mortality rate of phytoplankton, γ_1 is the fraction of total net primary production that is exuded by phytoplankton as DON, m is a quantity (units m d^{-1}) that parameterizes the diffusive mixing between the mixed layer and the deep ocean, and $h^+(t)$ has been defined above. It should be noted that the formulation of the last term of Eq. 2 assumes that the phytoplankton concentration below the mixed layer is zero. This may be a reasonable assumption in the winter, spring or autumn, but is obviously not true during the summer in areas where a deep chlorophyll maximum (DCM) develops. The model will therefore overestimate the export of phytoplankton, and perhaps bacteria and ammonium, by mixing and detrainment, in stratified situations where such conditions occur.

The daily averaged phytoplankton growth rate σ will be a function of the amount of photosynthetically active radiation (PAR) incident on a cell during the day, which in turn will be a function of time of the year, latitude, mixed layer depth, the light absorption properties of the water column, the characteristics of the phytoplankton photosynthesis-irradiance relationship, and the nature of the nutrient limitation of cell growth. If it is assumed that light and nutrient limitation of growth are independent effects then we can write,

$$\sigma = J(t, M)Q(N_n, N_r) \tag{3}$$

where J is the light limited growth rate and Q is a nondimensional nutrient limiting factor. Evans and Parslow (1985) calculated J by assuming that the time a particular cell spends at a given depth is long compared to the photosynthesis reaction time, but short compared to the cell division time. In this case the total daily growth rate

averaged over the mixed layer depth can be written as,

$$J(t, M) = 2\frac{1}{M}\int^{\tau}\int^{M} F(I_0(t)\exp^{-(k_w+k_cP)z})\,dzdt \tag{4}$$

where $F(I)$ is a function describing the phytoplankton photosynthesis-irradiance relationship (the P-I curve), 2τ is the day-length, $I_0(t)$ is the PAR immediately below the surface of the water, k_w is the light attenuation coefficient due to water (assumed to be constant with depth), and k_c is the phytoplankton self-shading parameter. Given data on $I_0(t)$ and a choice of the function $F(I)$ it is possible to calculate the integral in Eq. 4 numerically. However, Evans and Parslow (1985) showed that if the Smith function (Smith, 1936), given by

$$F(I) = \frac{V_p\alpha I}{(V_p^2 + \alpha^2 I^2)^{1/2}} \tag{5}$$

(where V_p is the growth rate as $I \rightarrow \infty$ and α is the initial slope of the *P-I* curve) is chosen, and if the variation of $I_0(t)$ with time of day is assumed to be triangular, then it is possible to obtain an analytical integration of Eq. 4. The resulting expression for J involves the parameters α, V_p, k_w, k_c, τ, M, and $I_n(t)$ the PAR just below the surface at noon (Evans and Parslow, 1985).

To define the nutrient limitation factor Q, the familiar Michaelis-Menten equation has been used to parameterize the effect of nutrient concentration on nutrient uptake and therefore, assuming balanced growth, on growth rate (Jamart *et al.*, 1977; Wroblewski, 1977; Fasham *et al.*, 1983). As our model distinguishes between nitrate and ammonium it is desirable to allow phytoplankton cells to take up ammonium preferentially, resulting in nitrate uptake being inhibited in the presence of significant concentrations of ammonium (Walsh and Dugdale, 1972; Glibert *et al.*, 1982). We have used the parameterization proposed by Wroblewski (1977) in which

$$Q(N_n, N_r) = Q_1(N_n, N_r) + Q_2(N_r) = \frac{N_n e^{-\Psi N_r}}{K_1 + N_n} + \frac{N_r}{K_2 + N_r} \tag{6}$$

where K_1, K_2 are the half-saturation constants for nitrate and ammonium uptake respectively, and Ψ is a constant that parameterizes the strength of the ammonium inhibition of nitrate uptake.

d. The zooplankton equation. The zooplankton are assumed to graze phytoplankton, bacteria and detritus and the equation can be written as,

$$\frac{dZ}{dt} = \beta_1 G_1 + \beta_2 G_2 + \beta_3 G_3 - \mu_2 Z - \mu_5 Z - h(t)\frac{Z}{M} \tag{7}$$

where G_1, G_2, G_3 are the grazing rates of zooplankton on phytoplankton, bacteria and detritus respectively, β_1, β_2, β_3 are the equivalent assimilation efficiencies, μ_2 is the zooplankton specific excretion rate, and μ_5 is the specific mortality rate. Note that as discussed in Section 2b the function $h(t)$ and not $h^+(t)$ is used to describe the effect of mixed layer changes on zooplankton, and that zooplankton are assumed to be sufficiently motile to be unaffected by diffusive processes.

A Michaelis-Menten equation was used to parameterize the effect of food levels on grazing rate. Firstly a measure of total food, F, is defined as

$$F = p_1P + p_2B + p_3D \tag{8}$$

where p_1, p_2, p_3 are measures of the zooplankton preferences for the various food types. The grazing rate on, for example, phytoplankton is then defined as,

$$G_1 = gZ \frac{p_1P}{K_3 + F} \tag{9}$$

where g is the maximum specific grazing rate, and K_3 is the half-saturation constant for grazing. Equivalent equations can be written for G_2 and G_3 such that the total zooplankton grazing $G_1 + G_2 + G_3$ will equal $gZF/(K_3 + F)$.

The relationship between total grazing and the concentration of the various food items will depend on the precise formulation chosen for the preferences. This complex issue is discussed in Appendix A where it is argued that, in order to effectively model zooplankton feeding, the preferences should be functions of the relative prey density. Such a choice results in the following expression for G_1,

$$G_1 = \frac{gZp_1P^2}{K_3(p_1P + p_2B + p_3D) + p_1P^2 + p_2B^2 + p_3D^2} \tag{10}$$

with analogous expressions for G_2 and G_3.

There is abundant experimental evidence that zooplankton excrete both ammonium and DON, although there has been some controversy about the relative importance of the two forms (Johannes and Webb, 1965; Corner and Newell, 1967). Another possible source of DON is from cell breakdown of food items during messy feeding by zooplankton (Roy *et al.*, 1989). These processes have been parameterized by assuming that a fraction ϵ of the zooplankton excretion is in the form of ammonium and $1 - \epsilon$ in the form of DON.

Finally the fate of the dead zooplankton needs to be discussed. It might be argued that dead zooplankton simply become detritus and are then subsequently broken down to DON or sink out of the mixed layer. However, it must be remembered that part of the zooplankton mortality is a model closure term representing the predation on zooplankton by higher predators which are not explicitly modelled. The final destination of such dead zooplankton will be either ammonium, fecal pellets, or dead higher predators. The fecal pellets and corpses of the higher predators will have high sinking

rates and will therefore sink out from the mixed layer on time-scales which are small compared to the other processes in the model. The simplest way to parameterize this whole process is, therefore, to assume that a fraction Ω of the mortality is instantly exported from the mixed layer and a fraction $1 - \Omega$ is converted into ammonium.

e. The Bacteria equation. Bacteria are assumed to take up ammonium and DON and also excrete ammonium. However, DON and ammonium are not equally interchangeable forms of nitrogen for bacteria. Bacteria obtain their carbon from DON and are thought to take up ammonium mainly to obtain sufficient nitrogen to synthesize cell protein. Therefore, in a balanced growth situation, the ammonium uptake will depend on the C/N ratio of the DON and bacteria, and the bacterial gross growth efficiency (GGE) for nitrogen and carbon (Fenchel and Blackburn, 1979; Goldman *et al.*, 1987; Ducklow *et al.*, 1989). In order to quantify this concept we define the bacterial uptake of ammonium and DON as e and d respectively. If the carbon/nitrogen ratios of bacteria and DON are defined as R_b and R_d respectively, and the bacterial *GGE* for carbon and nitrogen are g_c and g_n respectively, then the bacterial production h, in nitrogen units, will be given by,

$$h = g_n(e + d). \tag{11}$$

Similarly the bacterial production H, in carbon units, will be given by

$$H = R_b h = g_c R_d d. \tag{12}$$

Dividing Eq. 11 by 12 and rearranging we obtain,

$$\frac{e}{d} = \frac{g_c R_d}{g_n R_b} - 1. \tag{13}$$

In a balanced growth situation, the ratio of bacterial ammonium uptake to DON uptake should be constant in order to ensure that bacterial biomass of the required C/N ratio is produced from DON with a given C/N ratio. In this way DON can be made a proxy for DOC in the model. This concept can be incorporated into a Michaelis-Menten model of bacterial uptake (G. T. Evans, pers. comm.) by first defining a total bacterial nitrogenous substrate S as

$$S = \min (N_r, \eta N_d) \tag{14}$$

where $\eta = (g_c R_d / g_n R_b) - 1$. Then the bacterial DON uptake (U_1) and ammonium uptake (U_2) can be written as,

$$U_1 = \frac{V_b B N_d}{K_4 + S + N_d} \tag{15}$$

$$U_2 = \frac{V_b B S}{K_4 + S + N_d} \tag{16}$$

where V_b is the maximum bacterial uptake rate and K_4 is the half-saturation coefficient for uptake. This formulation ensures that the uptake of ammonium will be η times the DON uptake, as required by the balanced growth model, as long as there is sufficient ammonium present to meet this demand. However, if there is insufficient ammonium, the uptake rate of both DON and ammonium will be reduced accordingly.

The full equation for bacteria can now be written as,

$$\frac{dB}{dt} = U_1 + U_2 - G_2 - \mu_3 B - \frac{(m + h^+(t))B}{M} \tag{17}$$

where μ_3 is the bacterial specific excretion rate. Note that we have not attempted to parameterize separately bacterial mortality but have considered it to be subsumed within bacterial excretion.

f. The detritus equation. The detritus equation is given by,

$$\frac{dD}{dt} = (1 - \beta_1)G_1 + (1 - \beta_2)G_2 - \beta_3 G_3 - \mu_4 D + \mu_1 P - \frac{(m + h^+(t) + V)D}{M} \tag{18}$$

where μ_4 is the specific rate of breakdown of detritus to DON, V is the detrital sinking rate, and the other parameters have already been defined. The first two terms of this equation represent the fecal pellets derived from zooplankton grazing of phytoplankton and bacteria respectively. The third term represents the net loss of detritus by zooplankton grazing, i.e. $((1 - \beta_3)G_3) - G_3$. The fourth term represents the breakdown of detritus and fifth term represents the addition of dead phytoplankton to the detrital pool.

The breakdown of detritus to DON may be partly purely chemical leaching and partly due to bacterial activity. Therefore, strictly speaking this term should be some function of bacterial biomass. However, as already discussed, this would necessitate defining a separate attached bacterial compartment (see e.g. Pace *et al.*, 1984). In order to keep the model comparatively simple we have parameterized this process by a linear decay term.

g. The nitrate equation. The nitrate equation is,

$$\frac{dN_n}{dt} = -J(t, M)Q_1(N_n, N_r)P + \frac{(m + h^+(t))}{M}(N_0 - N_n) \tag{19}$$

where N_0 is the nitrate concentration below the mixed layer which is assumed to be constant. The first term is the new primary production which, in near steady-state conditions such as during the summer, will be balanced by the diffusive mixing of nitrate across the thermocline. However, as will be shown below, at other times of the

year nitrate fluxes due to changes in mixed layer depth will greatly exceed those due to diffusive mixing.

h. The ammonium equation. The ammonium equation is,

$$\frac{dN_r}{dt} = -J(t, M)Q_2(N_r)P - U_2 + \mu_3 B + (\epsilon\mu_2 + (1 - \Omega)\mu_5)Z - \frac{(m + h^+(t))}{M} N_r. \tag{20}$$

The first two terms represent the uptake of ammonium by phytoplankton (regenerated primary production) and bacteria respectively, the second represents the excretion by bacteria and the third represents the addition from zooplankton excretion and remineralization of grazed zooplankton by unmodelled higher predators. It should be noted that we have assumed that the ammonium concentration below the mixed layer is zero. There have been many observations of ammonium maxima below the thermocline in ice edge and upwelling regions at certain times of the year (Smith *et al.*, 1985; Murray *et al.*, 1989), but few we are aware of in the open sea. Nonetheless, this assumption is difficult to justify. However without explicitly modelling the biological processes in the thermocline it is difficult to assign any particular constant value for the submixed layer ammonium concentration that would hold for the whole year.

i. The dissolved organic nitrogen equation. The DON equation is

$$\frac{dN_d}{dt} = \gamma_1 J(t, M)Q(N_n, N_r)P + \mu_4 D + (1 - \epsilon)\mu_2 Z - U_1 - \frac{(m + h^+(t))}{M} N_d. \tag{21}$$

The first three terms represent the production of DON by phytoplankton exudation, detrital breakdown, and zooplankton excretion and messy feeding respectively, while U_1 is the uptake of DON by bacteria. As was the case for ammonium, we have assumed that the labile DON concentration below the mixed layer is zero; there is very little observational information to justify assuming otherwise.

3. Choice of parameters.

The model equations contain 27 parameters which, together with the values assigned to them for the standard run, are listed in Table 1. The assignment of values for biological parameters is especially difficult as, unlike many chemical or physical parameters, they cannot strictly be regarded as constants. We have approached this problem by using the model to predict the seasonal cycle of nitrogen for Bermuda station "S", for which there exists a comparatively large amount of physical and biological data. Where possible, therefore, we have chosen parameter values derived from observations made at this station or from other areas with similar oceanographic

Table 1. Model parameters.

Parameter	Symbol	Value
PAR/Total Irradiance	—	0.41
Cloudiness	—	4 Oktas
Light attenuation due to water	k_w	0.04 m^{-1}
Cross-thermocline mixing rate	m	0.1 m d^{-1}
Phytoplankton maximum growth rate	Vp	2.9 d^{-1}
Initial slope of P-I curve	α	0.025 $(W\ m^{-2})^{-1}\ d^{-1}$
Half-sat for Phy nutr. uptake	K_1	0.5 mMol m^{-3}
Phy. specific mortality rate	μ_1	0.045, 0.09 d^{-1}
Light atten. by phytoplankton	k_c	0.03 m^2 $(mMol\ N)^{-1}$
Phy. Exudation fraction	γ_1	5%
NH_4 inhibition parameter (Phy)	Ψ	1.5 $(mMol\ N)^{-1}$
Zooplankton maximum growth rate	g	1.0 d^{-1}
Zoop. assimilation efficiency	$\beta_1, \beta_2, \beta_3$	75%
Zoop. specific excretion rate	μ_2	0.1 d^{-1}
Zoop. specific mortality rate	μ_5	0.05 d^{-1}
Zoop. half-sat. for ingestion	K_3	1.0 d^{-1}
Detrital fract. of Z mortality	Ω	33%
Ammonium fract. of Z excretion	ϵ	75%
Bacterial maximum growth rate	V_b	2.0 d^{-1}
Bact. specific excretion rate	μ_3	0.05 d^{-1}
Bact. half-sat. rate for uptake	K_4	0.5 mMol N m^{-3}
NH_4/DON uptake ratio	η	0.6
Detrital breakdown rate	μ_4	0.05 d^{-1}
Detrital sinking rate	V	1, 10 m d^{-1}

conditions. However, parameters for which no good observational data exist (for example, phytoplankton natural mortality rate) were regarded as free parameters that could be varied in an attempt to match the modelled seasonal cycles of primary production, phytoplankton and nitrate to the observations obtained by Menzel and Ryther (1960).

In any such exercise it obviously helps to have some knowledge of the sensitivity of the model to the parameter values. The procedure used (see Appendix B) was to test the sensitivity of each parameter in turn by running the model to a steady-state with the parameter altered first to a higher and then to a lower value. In this way it was possible to determine which parameters had the most effect on which variables. The sensitivity was quantified by calculating a normalized sensitivity defined as the percentage change in a variable produced by a percentage change in the parameter. Sensitivities for annual net primary production (ANPP) and annual *f*-ratio (annual new production divided by ANPP) are given in Table 2.

a. Physical parameters. The main physical forcings in the model are the annual cycles of mixed layer depth and solar radiation. Daily mixed layer depths for Bermuda were

Table 2. Normalized parameter sensitivity of annual NPP and annual F-ratio for each parameter (see text for definitions).

Parameter	Standard value	Parameter range	Normalized sensitivity: Annual NPP	Normalized sensitivity: Annual F
Cloudiness	4	3, 5	−0.1, −0.2	0.1, 0.1
Attenuation coefficient for water (k_w)	0.4	0.038, 0.051	−1.6, −1.1	0.8, 0.4
Atten. coeff. for phytoplankton (k_c)	0.03	0.02, 0.04	−0.2, −0.2	0.1, 0.1
PAR/total fraction	0.43	0.5	1.4	−0.7
P-I curve initial slope (α)	0.025	0.0175, 0.05	1.3, 0.8	−0.5, −0.4
Phytoplankton uptake rate (V_p)	2.9	2.3, 3.4	0.4, 0.3	−0.2, −0.1
Zooplankton ingestion rate (g)	1.0	0.9, 2.0	0.4, 0.2	−0.6, −0.3
Bacterial uptake rate (VB)	2.0	1, 3	0.02, 0.06	−0.02, −0.06
Zooplankton egestion fraction (1-b)	0.25	0.1, 0.3	−0.4, −0.2	0.4, 0.2
Phytoplankton exudation fraction (γ_1)	0.05	0.024, 0.1	−0.1, −0.1	0.02, 0.01
Zooplankton excretion rate (μ_2)	0.10	0.05, 0.12	−0.1, −0.2	0.3, 0.3
Bacterial excretion rate (μ_3)	0.05	0.025, 0.1	0.1, 0.1	−0.1, −0.1
Phytoplankton mortality rate (μ_1)	0.09	0.045, 0.11	−1.5, −1.1	0.7, 0.4
Zooplankton mortality rate (μ_5)	0.05	0.025, 0.07	−0.5, −0.1	0.4, 0.2
Detrital breakdown rate (μ_4)	0.05	0.025, 0.1	0.3, 0.2	−0.4, −0.2
Detrital sinking rate (V)	1	0, 1.5	−0.5, −0.2	0.4, 0.2
Diffusion mixing rate (m)	0.1	0.05, 0.2	0.2, 0.2	−0.01, −0.04
Sub-mixed layer NO_3 conc. (N_0)	2	1.85, 3	1.7, 2.1	−0.7, −0.6
Phyto. uptake 1/2-sat. constant (K_1)	0.5	0.25, 0.75	−1.5, −0.6	0.7, 0.3
Zoopl. ingestion 1/2-sat. constant (K_2)	1	0.5, 1.2	−0.4, −0.2	0.5, 0.3
Bacterial uptake 1/2-sat. constant (K_3)	0.5	0.25, 1.0	0.01, −0.0	0.01, 0.01
NO_3 inhibition parameter (Ψ)	1.5	0.75, 3	−0.4, −0.3	0.2, 0.1
Ratio bacterial NH_4 to DON uptake (η)	0.6	0.3, 1.2	−0.1, −0.1	0.1, 0.05

obtained by interpolating from monthly means (Levitus, 1982; using the density criterion for mixed layer depth). The resulting seasonal cycle is plotted in Figure 2, together with observed values for the years 1958–60, derived from temperature profiles from Bermuda station 'S' (Bermuda Biological Station, 1960). On the whole the Levitus mixed layer depths are a good fit to the observations, although there is a suggestion that they underestimate the mixed layer in winter.

The annual variation in solar radiation is specified in the model by the function $I_n(t)$, the PAR just below the water surface at noon. For any given latitude and date $I_n(t)$ can

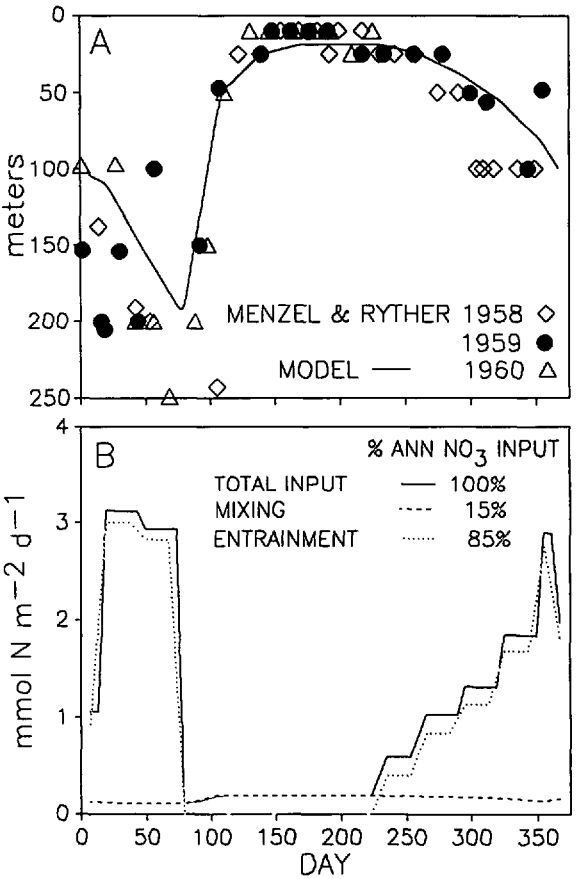

Figure 2. Annual cycles of (a) mixed layer depth and (b) NO_3 input for the model, with observed mixed layer depths recalculated from the data of Menzel and Ryther (Bermuda Biological Station, 1960).

be calculated from the standard astronomical formulae (Brock, 1981), the cloud cover, the ratio of PAR to total solar irradiance, and the transmittance at the water surface. The mean total cloud cover in the region of Bermuda is 4 oktas with an annual range of 1 okta (Isemer and Hasse, 1985). A variation of one okta does not have a significant effect on model results (Table 2) and so a constant value of 4 oktas was assumed. The effect of cloud cover on atmospheric transmittance was calculated using the equation proposed by Smith and Dobson (1984). The ratio of PAR to total irradiance is affected by sun zenith angle, water vapor content and aerosol optical thickness (Baker and Frouin, 1987). However, such refinements are outside the scope of the present model and so a constant value of 0.43 for the ratio was adopted (Jerlov, 1976; Jitts *et al.*, 1976). A value of 0.96 was assumed for the transmittance at the air-water interface (Smith and Baker, 1987).

According to Jerlov (1976) the Sargasso Sea waters are oceanic type I, which are characterized by a 1% light level depth of 105 m or an equivalent k_w of 0.044 m^{-1}. However, the Jerlov data includes the effect of phytoplankton absorption. Lorenzen (1972) suggested a k_w of 0.038 for water containing no phytoplankton and we have used a rounded value of 0.04 m^{-1}. The sensitivity analysis showed that k_w was one of the more critical parameters and so in cases where good data are available it would be worth using a more accurate parameterization of light absorption (Fasham *et al.*, 1983).

The diffusion of nitrate across the thermocline is controlled by the diffusion rate, m, and the nitrate concentration below the mixed layer, N_0. m was set at 0.1 m d^{-1}, which is approximately equivalent to a vertical diffusion coefficient of 0.3 cm^2 s^{-1} across a 20 m thermocline. The determination of an unambiguous value of N_0 presents some problems because the model assumes a step gradient of nitrate at the base of the mixed layer, whereas in reality there is a nitracline of varying vertical extent. The data of Menzel and Ryther (1960; see Figure 5) would suggest an N_0 value of between 1 and 2 nMol N m^{-3} depending on the time of the year and a value of 2 mMol N m^{-3} was adopted (see next section for a fuller discussion of the reasons for this choice).

This simple approach to modelling nitrate diffusion will probably be in error during the summer months for areas, such as Bermuda, where a deep chlorophyll maximum (DCM) develops. Such a DCM may act as a trap cutting off much of the diffusive transport of nitrate into the mixed layer. In comparison, the model will tend to overestimate new production and f-ratio during the summer.

b. Phytoplankton parameters. The empirical relationship between phytoplankton maximum growth rate and temperature derived by Eppley (1972) was used to assign a value for the phytoplankton maximum growth rate V_p. The range of mixed layer temperatures at Bermuda station "S" is 21–27°C (Menzel and Ryther, 1960) giving growth rates between 2.3 and 3.4 d^{-1} using the Eppley formula. Differences in V_p of this magnitude would only produce a 6% change in ANPP (Table 2) and so a mean value of 2.9 d^{-1} was assumed for all runs.

The initial slope of the P-I curve, α, is a very sensitive parameter (Table 2). Luckily, there has been a reasonable number of measurements of this quantity made in the Sargasso Sea area by T. Platt's group at Bedford Institute of Oceanography. The data range from 0.039 to 0.70 mgC (mg Chl a)$^{-1}$ h^{-1} (W m^{-2})$^{-1}$ with a mean value of 0.05 (T. Platt, pers. comm.). A carbon/chlorophyll ratio of 50 was used to calculate an equivalent α value of 0.025 d^{-1} (W m^{-2})$^{-1}$.

Bannister (1974) made a critical assessment of previous determinations of k_c, the light attenuation due to chlorophyll, and suggested a value of 0.016 m^2 (mg Chl a)$^{-1}$. Fasham *et al.* (1983) obtained a mean value of 0.026 by correlating light and chlorophyll profiles. k_c is not a sensitive parameter and so a mean value of 0.02 was adopted and converted from biomass units of chlorophyll to nitrogen by assuming a

carbon/chlorophyll ratio of 50 and a Redfield C/N ratio of 6.625, giving a value of 0.03 m^2 (mMol N)$^{-1}$.

A value of 0.5 mMol N m^{-3} was chosen for the half-saturation parameter for phytoplankton nitrate uptake, K_1, which is representative of experimental observations (Goldman and Glibert, 1983), although values as low as 0.1 have been suggested. The difficulty in measuring low levels of NH_4 has recently been resolved (Brzezinski, 1987), but to date, there are no published results for kinetic determinations employing this method. In the absence of good experimental data the half-saturation constant for ammonium uptake, K_2, was given the same value as K_1. Wroblewski's (1977) estimate of 1.5 (mMol N m^{-3})$^{-1}$ was used for the nitrate uptake ammonium inhibition parameter.

The parameter γ_1 is the fraction of the primary production that is exuded from the phytoplankton cells in the form of DON. It is often assumed that 5–15% of carbon production is exuded as DOC (Sharp, 1977). However, the equivalent fraction for DON exudation is not so well documented although, as the C/N ratio of the exudation products is thought to be high compared to particulate production (Fogg, 1983; Lancelot and Billen, 1986), the fraction is likely to be less than for carbon. We assumed a rather conservative value of 5% for γ_1 (Schell, 1974).

The phytoplankton specific mortality rate, μ_1, is the most sensitive model parameter (Table 2) and yet it is the most difficult to determine. There are no extant estimates of μ_1 yet, as Walsh (1983) concluded, phytoplankton mortality and subsequent sinking may be the most important loss term in many, if not all marine systems. It was therefore decided to use μ_1 as a free parameter that could be adjusted to yield a required ANPP for any given choice of the remaining parameters. This process will be described more fully in the section.

c. Zooplankton parameters. The assignment of parameter values for zooplankton also presents some problems because, as discussed previously, the zooplankton compartment models an animal which is a combined herbivore, bacteriovore and detritivore. We have chosen parameters that are more typical of the herbivorous copepod part of this 'portmanteau' animal than the bacterivorous flagellate part. The chosen values for maximum growth rate g (1.0 d^{-1}) and half-saturation constant for ingestion K_3 (1.0 mMol N m^{-3}) were the same as used by Evans and Parslow (1985), but a higher zooplankton assimilation efficiency (β) of 75% was adopted (Conover, 1978).

The zooplankton specific mortality rate, μ_5, parameterizes both natural and predator mortality. Evans and Parslow (1985) used a value of 0.07 d^{-1}, while Wroblewski *et al.* (1988) used 0.2 d^{-1}. As was the case of phytoplankton, observational data on this parameter are rare. Riley (1947) used a time series of zooplankton and phytoplankton concentrations from the Georges Bank to estimate zooplankton loss rates, which varied from around 0.01 d^{-1} to 0.05 d^{-1} throughout the year. A recent re-analysis of these

data suggested even higher values at certain times of the year (Davis, 1987). We used a value of 0.05 d^{-1} for all runs.

The parameter Ω, the fraction of zooplankton mortality going to ammonium, was estimated by assuming that the model zooplankton mortality is the input to an infinite series to higher predators. If it is assumed that all these higher predators have a gross growth efficiency of 25% and an assimilation efficiency of 75% then, by summing the series to infinity, it is simple to show that Ω is $\frac{1}{3}$ (see e.g. King, 1987).

Verity (1985) has reported mass-specific excretion rates for a number of oceanic copepods and the mean of these values was 0.15 d^{-1}. However, initial simulations showed that using such a high value, in conjunction with a mortality rate of 0.05 d^{-1}, resulted in the zooplankton going extinct in the winter. A lower value of 0.1 d^{-1} was therefore adopted. It was assumed that 75% of the zooplankton excretion was in the form of ammonium and 25% DON (Corner and Newell, 1967). Less excretion as DON results in bacterial production which is too low (see below).

d. Bacteria and detritus parameters. A maximum bacterial uptake rate, V_b, of 2.0 d^{-1} was chosen as representative of oceanic bacteria (Ducklow and Hill, 1985). Estimates of the half-saturation parameter K_4 were obtained from Carlucci *et al.* (1985) and Fuhrman *et al.* (1987). Reliable estimates of the specific excretion rate μ_3 are not available for bacteria. However, the magnitude of excretion will affect the GGE of the bacteria, and so an excretion rate of 0.05 d^{-1} was chosen which gave reasonable bacterial GGE's throughout the seasonal cycle. The parameter η measures the ratio of bacterial uptake of ammonium to DON (Eq. 14) and its magnitude depends on the bacterial GGE for carbon and nitrogen and the C/N ratios for bacteria and DON. We have assumed that the two GGE's are equal and that the C/N ratios of bacteria and DON are 5 (Fenchel and Blackburn, 1979) and 8 (Suzuki *et al.*, 1985) respectively, yielding a value for η of 0.06.

Two parameters are required for the detritus compartment, the sinking rate and the rate of breakdown to DON. Detritus is comprised of a variety of components of varying sizes and sinking rates and this makes the determination of a single sinking rate extremely problematic. We have circumvented this problem by running the model with two different sinking rates of 1 and 10 m d^{-1} and investigating the different seasonal cycles that were produced. We also ran some simulations with a sinking rate of 100 m d^{-1} but found that, apart from bacteria and detritus, the results were similar to those for the 10 m d^{-1} case. Jones and Henderson (1986) have reviewed the breakdown rates of dead organic matter and found them to lie between 0.004 and 0.18 d^{-1}; we used a value of 0.05 d^{-1} which, as will be discussed below, gave reasonable values of bacterial production.

e. Numerical methods. The full set of differential equations were solved using a fourth-order Runge-Kutta algorithm. Some initial experiments were carried out with

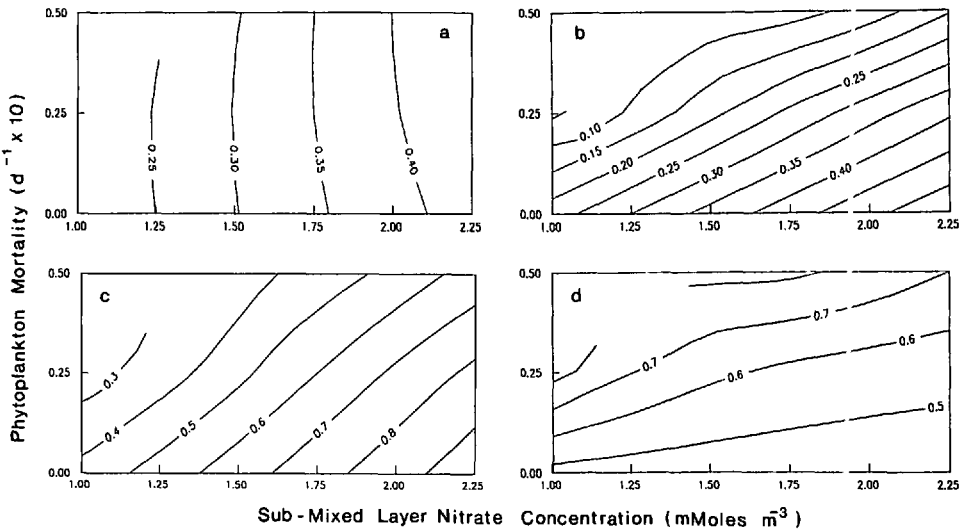

Figure 3. Contours of modelled (a) annual new production, (b) annual regenerated production (c) annual total primary production (all in mMol N m^{-2} y^{-1}), and (d) annual *f*-ratio as functions of phytoplankton specific mortality rate and submixed layer nitrate concentration (N_0). The detrital sinking rate for these simulations was 10 m d^{-1} with the other parameter values as specified in Table 1.

different integration time steps and it was found that a time step of 1 day was sufficient to give accurate estimates of the state variables. However, for the purpose of calculating annual budgets it was found that a time step of 0.2 days was needed to give a flow network which was balanced to a 1% accuracy.

The simulations were run until a steady-state annual cycle was achieved, i.e. the state-variable concentrations on a given day of the year were the same in successive years of the simulation. The model is not very sensitive to initial conditions and it usually took about 3 years to achieve a steady-state.

4. Comparison of model results with data from Bermuda Station "S"

In the previous section it was observed that the phytoplankton specific natural mortality rate could not be estimated reliably and that it was difficult to assign a value for N_0 that would be appropriate for the whole seasonal cycle. It was decided, therefore, to use these as free parameters for fitting the model to Bermuda Station "S" data. Contours of modelled new, regenerated, and total annual primary production, and annual *f*-ratio (the ratio of annual new to total primary production) as functions of phytoplankton mortality and N_0 are plotted in Figure 3 (these results were obtained using the standard model parameters (Table 1) and a detrital sinking rate of 10 m d^{-1}). These contours show that new production is almost entirely controlled by N_0 (Fig. 3a), but that both parameters have an effect on the regenerated and total production (Figs.

3b and 3c). Regenerated production decreases with increased phytoplankton mortality because increased natural mortality results in more primary production flowing into detritus, rather than zooplankton. Although some of this detrital flux can be recycled back to the phytoplankton via detrital breakdown and bacterial uptake and ammonium excretion, this recycling route is less efficient than recycling via zooplankton ammonium excretion resulting in a lower regenerated production. The differential effect of phytoplankton mortality on new and regenerated production means that, for any given value of N_0, the annual f-ratio will increase with increasing mortality (Fig. 3d). Phytoplankton mortality and N_0 can, therefore, be used to adjust the modelled new and total annual primary production to given values, but the modelled f-ratios will also be affected.

The ^{14}C measurements made between 1958 and 1960 at Bermuda Station "S" were used to derive an annual net total primary production (ANPP) value for calibrating the model. Menzel and Ryther (1960) have summarized these data and estimated that the average daily net primary production for 1958 was 0.2 gC m^{-2} d^{-1} giving an annual total of 72 gC m^{-2} yr^{-1}. However, this production estimate is not the appropriate value for calibrating the model because it includes the summer production in the DCM, below the mixed layer. Therefore, the original data sheets (Bermuda Biological Station, 1960) were used to calculate the vertically integrated production, both over the whole vertical range of observations and within the mixed layer only, for each day that the station was occupied. These daily integrated values were then integrated over the whole year, using a trapezoidal integration, to give estimates of ANPP. The result for 1959 (the only full year with complete coverage) was an ANPP of 62.9 gC m^{-2} y^{-1} for the total euphotic zone and 46.1 gC m^{-2} y^{-1} for the mixed layer alone, or 0.58 Mol N m^{-2} y^{-1} assuming a Redfield ratio of 6.625. New production is of the order 3 Mol C m^{-2} y^{-1} (0.45 Mol N m^{-2} y^{-1}) at Station "S" (Jenkins, 1988) implying an annual f ratio of 0.78, which is much higher than estimates derived from the nitrate observations (Platt and Harrison, 1985) and has led some workers to suggest that the ^{14}C technique underestimates primary production (Jenkins and Goldman, 1985).

A model ANPP of 0.58 Mol N m^{-2} y^{-1} can be achieved using an N_0 value in the range 1.35–2.25 with a suitable choice of mortality (Fig. 3c). However, to achieve such a value of ANPP and also a new production value of 0.45 Mol N m^{-2} y^{-1} would require an N_0 greater than 2.0 Mol N m^{-3} (Figs. 3a and 3b) and a phytoplankton mortality greater than 0.05 d^{-1}. The Menzel and Ryther (1960) nitrate data do not lend support to an N_0 value greater than the 2 mMol N m^{-3} and so it was decided to fix N_0 at 2 mMol N m^{-3} and adjust phytoplankton mortality to give the required value of ANPP. The final adopted values for phytoplankton mortality were 0.09 d^{-1} and 0.045 d^{-1} for the 1 m d^{-1} and 10 m d^{-1} sinking rates respectively.

For comparison, observed mixed layer nitrate and chlorophyll *a* concentrations were calculated by taking averages of all the observations made within the mixed layer for all the days for which the station was occupied. The phytoplankton values were

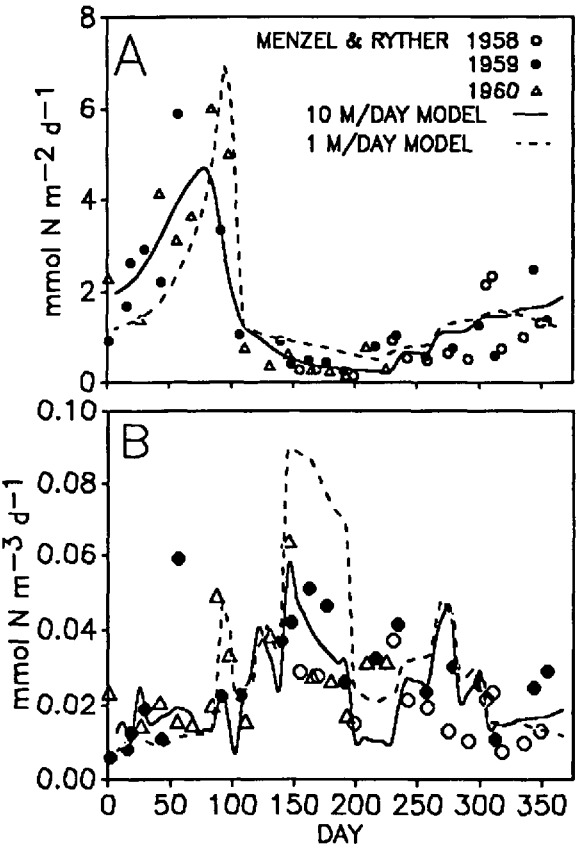

Figure 4. Comparison of observed data from Menzel and Ryther (Bermuda Biological Station, 1960) with model output for (a) areal and (b) volumetric primary production (NPP) over the annual cycle (lines and symbols as in (a)). The Bermuda data were recalculated to reflect mixed layer values only.

converted to nitrogen units using a carbon/chlorophyll ratio of 50 and a carbon/nitrogen ratio of 6.625.

Figure 4a shows the simulated seasonal cycles of vertically integrated (areal) mixed layer NPP, for the two detrital sinking rates, compared with the Station "S" data. The 10 m d^{-1} simulation appears to give a better overall fit to the observations, especially during the early part of the year and during the summer. An attempt was made to quantify the differing fits of the two simulations to the data by calculating a root-mean-square difference (RMSQD), defined as the square root of the sum, over the whole data set (1958–1960), of the squared differences between observed and modelled values (Wallach and Goffinet, 1989). The RMSQD values were 0.97 and 0.77 for the 1 and 10 m d^{-1} cases respectively, which confirms the purely visual assessment of the goodness-of-fit. However, the standard errors of the RMSQD values (Wallach and

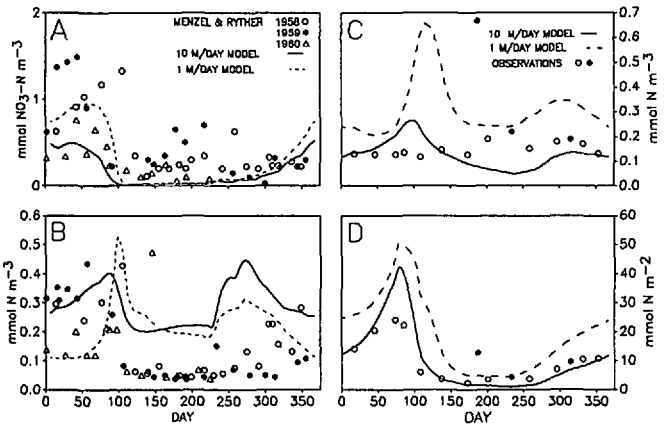

Figure 5. (a) and (b) as in Figure 4, for nitrate and phytoplankton nitrogen biomass (recalculated from raw data on chlorophyll; see text). (c) and (d) comparison of observed and modelled bacterial biomass. Open circles: data collected by Bermuda Biological Station and H. L. Quinby. Solid circles: data from Fuhrman *et al.* (1989). Data from vertical profiles were averaged over the model mixed layer depth for volumetric data, then multiplied by that depth for areal estimates. (b) and (d) symbols and lines as in (a) and (c), respectively.

Goffinet, 1989) were larger than the mean values, and so the difference in the RMSQD values was not statistically significant. Both simulations reproduced well the late winter/early spring increase in NPP and the decline after day 100. However, during this period changes in the areal NPP are mainly determined by changes in mixed layer depth, which is a model input variable; this agreement cannot therefore be used to any great extent in validating the model. When observed and modelled volumetric NPP was compared (Fig. 4b) it was found that both simulations gave a good fit to the data in the early part of the year, that the 1 m d^{-1} simulation overestimated the production during the summer, and that both simulations tended to overestimate the production during the autumn deepening of the mixed layer.

There was considerable inter-annual variability in the Station "S" nitrate data (Fig. 5a) which makes any comparison with the simulations very problematic. The 1 m d^{-1} simulation appeared to fit the data better in the early part of the year and the RMSQD values confirmed that this simulation gave a better overall fit to the data. Neither simulation reproduced the high observed summer nitrate values. However, techniques for measuring low nitrate concentrations were not highly developed in the late fifties and sixties and more recent results suggest that summer nitrate levels are usually less than 0.1 mMol m^{-3} (Altabet, 1989), which would support the model results. Alternatively, the higher values may represent periods when vertical mixing was increased by storms, or passage through the area of eddies, resulting in higher mixed layer nitrate concentrations (Nelson *et al.*, 1989).

In their paper describing the Station "S" data, Menzel and Ryther (1960) plotted a schematic seasonal depth profile of chlorophyll *a*, which indicated that there was a

well-defined mixed layer spring bloom sometime between late-March and late-April with chlorophyll *a* concentrations in the range 0.5–1.0 mg m^{-3} (0.3–0.6 mMol N m^{-3}). However, apart from perhaps the year 1958, the raw data we have obtained do not support this interpretation (Fig. 5b). As with the nitrate data there is high inter-annual variability, but the general picture is of high values in the late winter and early spring followed by a decline to low summer values once the mixed layer has shallowed after day 100. There is also a tentative suggestion of higher values during the autumn deepening of the mixed layer, at least for 1958. The two simulated seasonal cycles of phytoplankton distribution are interesting in that they are qualitatively different. The 1 m d^{-1} simulation yielded a classic spring bloom with a maximum concentration of about 0.5 m mMol N m^{-3}, in rough agreement with the schematic picture of Menzel and Ryther (1960). However, the 10 m d^{-1} simulation showed a gradual increase in phytoplankton biomass throughout the late winter with no pronounced bloom, which is more in agreement with the raw data.

Both simulations greatly overestimated the phytoplankton biomass in the summer and autumn. We have carried out many trial simulations in an attempt to obtain lower summer phytoplankton levels, while maintaining the observed ANPP values, but with no success as yet. Bearing in mind that simulated NPP during this period was reasonably close to the observed values, especially for the 10 m d^{-1} simulation (Fig. 4), then one possible reason for this discrepancy could be seasonal variations in the chlorophyll/nitrogen ratio. The value used to convert the chlorophyll observations to nitrogen units was 1.6 which may be inappropriate for the summer period. A theoretical formulation for the effect of light and nutrients on the chlorophyll/nitrogen ratio has been discussed by Kiefer and Atkinson (1984). Their results would suggest that the ratio might be closer to 0.5 for summer nutrient levels of 0.1 mMol N m^{-3}. This would mean the summer phytoplankton observations being multiplied by around 3, which would bring them more in line with the model results. Unfortunately there are no good observations of chlorophyll/nitrogen ratios to be able to test this speculation. It was partly for this reason that we chose to calibrate our model using the direct comparison with primary production data, rather than converting modelled phytoplankton biomass to chlorophyll using some arbitrary factor.

Mean mixed layer bacterial biomass data derived from microscopic counts and the conversion factors given in Lee and Fuhrman (1988) are plotted as volumetric and areal stocks in Figure 5. Both model runs produce a bacterial bloom which follows, and is derived from, the phytoplankton bloom (see below). This bloom is apparent only in the areal data (Fig. 5d), but there is no evidence of springtime increases in mixed layer bacterial concentrations. Thus like the modelled phytoplankton, the modelled bacterial bloom is driven mainly by changes in mixed layer depth. However, the average levels of biomass in the 10 m/day run are within a factor of two of the observed values. It should be noted here, that these data were not available until quite recently, and so no attempt was made to calibrate the bacterial output beyond adjusting the detrital decomposition

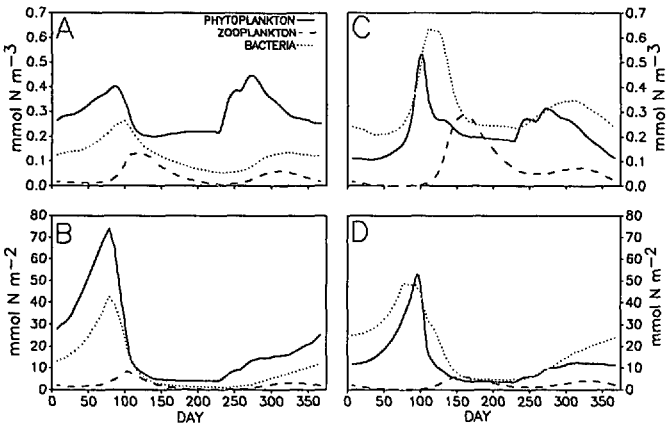

Figure 6. Model output for annual cycles of living biomass for (a,b) 10 m/day and (c,d) 1 m/day runs. Stocks are expressed as (a,c) mixed layer mean (volumetric) and (b,d) total mixed layer (areal) levels. Lines for b, c, d follow legend on Figure a.

rate and bacterial excretion rate to achieve an acceptable level of annual bacterial production. We believe that more realistic bacterial simulations will be achieved with a model including two size classes of zooplankton. A smaller bacterivorous size class with a faster response time suppresses the bloom shown in Figure 5c. In other respects, the model matches the existing data, including the observations of Fuhrman *et al.* (1989). It should also be noted that conversion of bacterial count data to biomass is still uncertain by a factor of nearly 10 (Lee and Fuhrman, 1988).

It is difficult to compare the simulated zooplankton cycles with observations as we know of no comprehensive seasonal sampling of zooplankton, across the whole size spectrum, at Station "S". Menzel and Ryther (1961) sampled the zooplankton concurrently with their other observations at Station "S". They used vertical net hauls (mesh size 360 μm) over a depth range of 0–500 m and reported zooplankton dry weights in the range 1.2–4.9 mg m^{-3}, with the highest values being observed in June. Deevey (1971) also used vertical nets (mesh size 200 μm) to sample the top 500 m at Station "S" during 1961–62, and found that dry weights ranged from 1.26–10.35 mg m^{-3}, with a mean value of 2.61 mg m^{-3}. With the exception of the high value of 10.35, which was observed in March, the other peaks in the time series were in May, June and August. Converting the Deevey data to nitrogen units gives a range of 0.009–0.073 mMol N m^{-3} with a mean of 0.018 mMol N m^{-3}. Be *et al.* (1971) carried out a program of zooplankton sampling throughout the North Atlantic and their results for the Bermuda area are in the range 0.04–0.07 mMol N m^{-3}. The simulated zooplankton concentrations (Fig. 6) are within these ranges throughout most of the year, but the peak values (10 m d^{-1} simulation: 0.14 mMol N m^{-3} on the 25th April; 1 m d^{-1} simulation: 0.29 mMol N m^{-3} on the 12th June) were much higher. One possible explanation for this discrepancy is that during this period there might be a high

population of microzooplankton which would not be sampled at all by conventional zooplankton nets. It should be remembered that the model zooplankton compartment is intended to encompass all size classes of zooplankton except the higher predators. Beers *et al.* (1982) found that in the top 200 m of the Pacific the biomass of zooplankton in the 2–200 μm size class was nearly 4 times that in the >200 μm size class. Bearing in mind that the nets used in the surveys referred to above would not adequately sample the 2–200 μm size class, then the observations of Beers *et al.* (1982) could explain the difference between model and data. Clearly, new data on microzooplankton stocks are important for further calibration of these models.

Like zooplankton, data for comparison with the remaining model compartments (NH_4, DON and detritus) are scarce. Most of the existing data on NH_4 and DON was collected with outmoded techniques which lacked the sensitivity needed to specify the low values expected for these compounds (Brzezinski, 1987, 1988; Fuhrman, 1987). Labile DON compounds such as dissolved free and combined amino acids are maintained at nanomolar levels by bacterial uptake (Fuhrman, 1987), and our results are consistent with this pattern (Fig. 7), though seasonal data are lacking. The same pattern holds for NH_4, for which concentrations less than the conventional detection limit (0.03 mMol m^{-3}), are the norm. Occasionally high levels do occur with no particular pattern apparent (Brzezinski, 1988). Our results show that NH4 is maintained at these levels in summer, but that higher concentrations occur in fall and winter, when bacterial regeneration of detritus is not balanced by phytoplankton uptake. As no wintertime sampling has been carried out, this prediction cannot yet be upheld or rejected out of hand.

In conclusion, the model was partially successful in fitting the observations for Bermuda Station "S" but, bearing in mind the possible inadequacies of the data, the simplicity of the food web model and the parameterization of physical mixing and mixed layer migration, it may be optimistic to expect a closer fit to the data.

5. Results

In our investigation of the dynamic behavior of this model we have examined over 200 different runs, in which different parameters have been varied to produce different results and to match the existing biogeochemical and ecological data on the Station S mixed layer more accurately. In this section, we describe and analyze some of the output from model runs 183 and 184. The parameters for these runs, and the rationale for choosing them were presented in the previous section. These runs compare two scenarios for the seasonal cycle at Bermuda; one in which the detrital material sinks from the mixed layer at a mean rate of 10 meters per day, and one with a detrital sinking rate of 1 m/day. There are several ways to consider these scenarios in the context of this simplified model. One is to assume that the modelled bulk particulate matter has a particle size (and mass) distribution which results in a mean sinking rate dominated by either larger or smaller-sized particles. Alternatively, these two contrast-

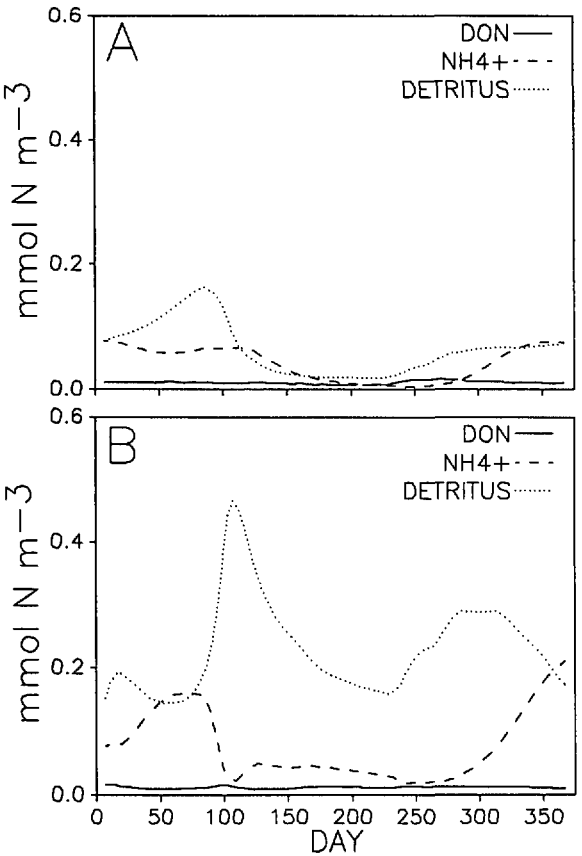

Figure 7. As in Figures 6ac, for nonliving biogenic Nitrogen (NH_4, DON, detritus), for both runs.

ing cases could be regarded as examples of plankton communities in which larger or smaller sized organisms dominated the standing stocks over the course of the annual cycles. We have also explored a run with a sinking rate of 100 m/day. The results for this run are about the same as the 10 m/day run for all compartments except detritus (as expected) and bacteria, which depend to a large extent on detrital breakdown in these runs.

In the following section we present first some of the bulk, or system-level results from the model output, comparing the results from the 1 and 10 m/day runs. Then some of the individual rate processes and the dynamics of individual compartments are examined in more detail, with the emphasis on the 10 m/day case. An important feature of our model is that it saves and integrates all of the intercompartmental flows shown in Figure 1. These are indispensable for analyzing the behavior of the stocks through the annual cycle, and for understanding the differences between runs. Such information on rate processes and their variability is also essential for understanding

the behavior and regulation of real plankton systems (Platt *et al.*, 1981; Moloney *et al.*, 1986).

a. System-level dynamics. Standing stocks. The dynamics of these models are driven by seasonal changes in mixed layer depth (Fig. 2a) which regulates the supply of PAR and NO_3 to the phytoplankton. The mixed layer cycle and our choice of submixed layer NO_3 concentration result in the cycle of NO_3 supply shown in Figure 2b. Nearly all the annual nitrate input (85%) is supplied by entrainment into the deepening mixed layer between days 225–365 and 1–75. Detrainment ceases abruptly when the mixed layer begins to restratify after day 75, and NO_3 input is limited to diffusion across the pycnocline during the summer.

Phytoplankton dominates the living biomass in the 10 m/d run (Figs. 5a, 6a), being always more abundant than either zooplankton or bacteria, which have peak abundances in the late spring and are lower the rest of the year. The standing stocks (areal mass per unit area for the entire mixed layer) show a different pattern (Fig. 6b,d). It is clear that most of the change in stocks for the bacteria and phytoplankton around day 100 is due to the rapid shoaling of the mixed layer, and the consequent loss (detrainment) of biomass which is left behind as the mixed layer rises. The model specified that the zooplankton are migratory and are not detrained. In the fall, nitrate is added (entrained) to the system as the mixed layer deepens (Fig. 2), resulting in accumulation of biomass from enhanced new production.

In the 1 m/day case (Figs. 5b, 6b), phytoplankton concentrations are lowest in the late winter with a pronounced bloom around day 100 which occurs slightly later than the 10 m/day case. Zooplankton stocks are higher in this run because they are sustained on detritus to a greater extent than in the rapid sinking rate case, where detritus is exported more rapidly. But the zooplankton build-up is entirely after the mixed layer has reached its shallowest depth, so the areal stocks never get very large. In the 10 m/day run, the zooplankton peak is earlier when the mixed layer is deeper, so although the concentration of zooplankton is low, the areal standing stocks are about the same as in the 1 m/day case. Bacterial stocks are also much higher in the 1 m/day run because of greater availability of detritus. In this run, bacteria exceed the phytoplankton biomass for most of the year (cf. Fuhrman *et al.*, 1989).

The nonliving biogenic stocks (NH_4, DON, detritus) are generally maintained at low levels throughout the year (Fig. 7), although detritus exhibits a spring "bloom" and exceeds the levels of zooplankton at that time. The 10 m/day run results in a system dominated by living matter throughout the year. The higher NH_4 concentrations in the 1 m/day run are derived from remineralization of the detritus (via bacterial metabolism) and zooplankton feeding and excretion. DON is kept well below the half-saturation concentration of 0.5 mMol N m^{-3} throughout the year, suggesting that the bacteria are always DON-limited.

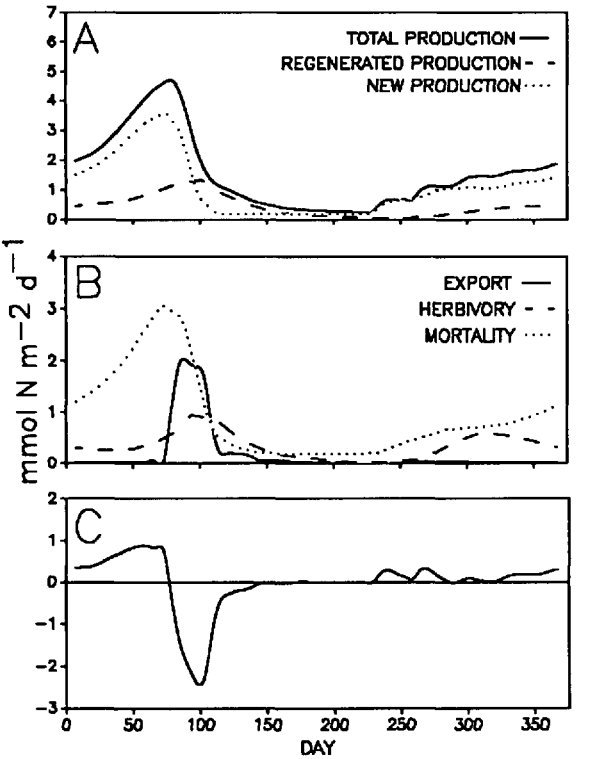

Figure 8. Annual cycles of phytoplankton dynamics for 10 m/day run. (a) Total net primary production, new production, and regenerated production. (b) Phytoplankton losses. (c) Net balance of mixed layer phytoplankton (production minus losses).

b. Primary production. The annual cycles for primary production are similar for the two cases (Figs. 8, 9), with a spring bloom already well along before the mixed later begins to shoal (cf. Fig. 2a). This suggests that at least for nitrogen, the onset of the bloom is forced more by the annual cycle of solar irradiance than by the mixing cycle at Bermuda. In the 10 m/day case, the bloom actually reaches its peak while the mixed layer is deepest. Primary production peaks later at a higher level in the 1 m/day case, possibly because nitrate declines more rapidly in the 10 m/day run.

The cycles for the components of primary production, new and regenerated production supported respectively by NO_3 and NH_4, are shown in Figs. 8a, 9a). The spring bloom is driven primarily by new production, which declines rapidly following the shoaling of the mixed layer, when the input of nitrate is limited to vertical diffusion (cf. Fig. 2b). Regenerated production exceeds new production (i.e., the f ratio is less than 0.5) for only a brief period between days 97–169 in the 10 m/day case (Fig. 12 inset), and is low during the rest of the year when zooplankton and bacterial stocks are low. Regenerated exceeds new production for a longer period in the 1 m/day case because

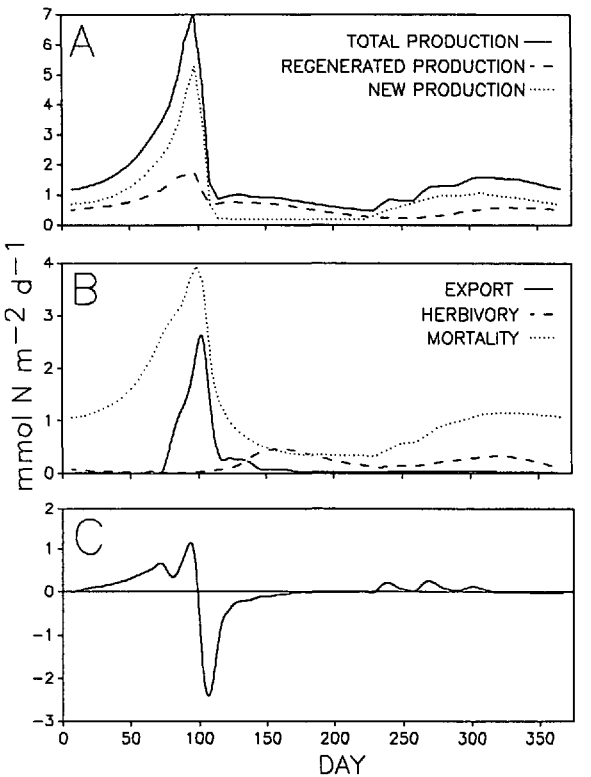

Figure 9. As in Figure 8, for 1 m/day run.

more nitrogen is conserved in the mixed layer. In this model, entrainment during mixed layer deepening is the principal source of nitrate.

c. Phytoplankton dynamics. Some idea of the factors controlling phytoplankton stocks can be gained from Figures 8bc, 9bc. Mortality (the flow of living phytoplankton biomass to detrital nitrogen) dominates the removal terms through most of the year. As suggested by the results in Figure 3, the interaction between mortality and sinking rate exerts a powerful control of phytoplankton dynamics. Export (including both entrainment and mixing) is an important sink for phytoplankton during the brief period when the mixed layer shoals. Herbivory is most important as a sink following the bloom, and is also high during the fall bloom period after day 250. The net gain or loss of phytoplankton biomass in the mixed layer is shown in Figures 8c, 9c. There are net gains (accumulation) of any importance only in the winter and early spring, when the mixed layer is deepening and entraining nitrate. A period of pronounced net removal follows the peak of the bloom. A period of nearly steady state conditions occurs during maximum stratification in summer though even very slight imbalances between gains and losses can result in substantial changes in the stocks over periods of days-weeks.

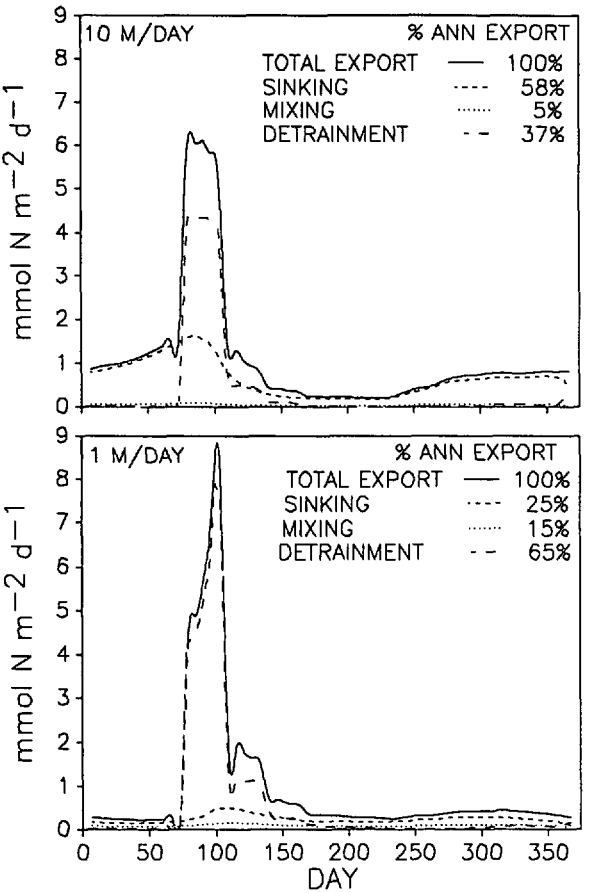

Figure 10. Annual cycles of export via detrainment, sinking and mixing (diffusion).

d. Exports and the sinking flux. There are three components of export from the mixed layer: the sinking flux of detrital particles, detrainment of materials when the mixed layer is shoaling, and mixing. In our model the concentrations of all stocks except nitrate are maintained at zero below the mixed layer, so mixing is never a source term (except for NO_3). Furthermore, the rates of detrainment and mixing would be lower if concentrations were nonzero below the mixed layer. Thus, in our model, the importance of mixing and detrainment are probably exaggerated, especially during summer, when levels of biogenic material is the pycnocline and lower euphotic zone may be high (e.g., during occurrence of the deep chlorophyll maximum). But during the rest of the year, especially after the DCM has been homogenized by deep mixing, our estimates may be more realistic.

Total export is relatively constant except during the period following the peak of the bloom when detrainment is maximal (Fig. 10). Most of the export is via detrainment at this time. In both cases, most of the export is particulate, because the dissolved stocks

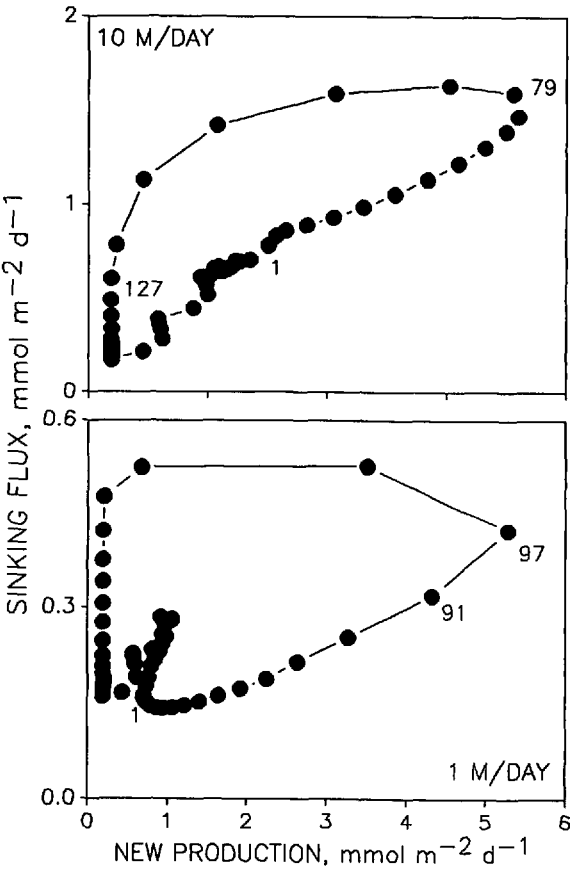

Figure 11. Annual cycles of sinking flux and new production, plotted as a phase diagram to show annual trajectory and covariance of input and export via detrital sedimentation. Numbers are days of model year.

are usually low, and do not sink. Particle sinking dominates the export during the rest of the year and reaches its annual peak during maximum detrital concentrations. Sinking is more important in the 10 m/day case, accounting for 58% of the annual export of biogenic stocks, compared to only 25% in the 1 m/day case. Thus it is interesting to relate sinking flux to new production (Fig. 11). In the 10 m/day case, the two fluxes are well-correlated except during days 79–127, when sinking is less important as a fraction of the total export. Sinking is less important in the 1 m/day run and the correlation between sinking and new production is less clear. These results suggest that if measurements of new production and vertical export of sinking particles can be carried out without bias at the correct scales (ca 1–10 days), then correlations between these processes should be observed (cf. Pace *et al.*, 1987). However, if other mechanisms besides sinking of large particles contribute to export, then the correlations should not be expected (Altabet, 1989).

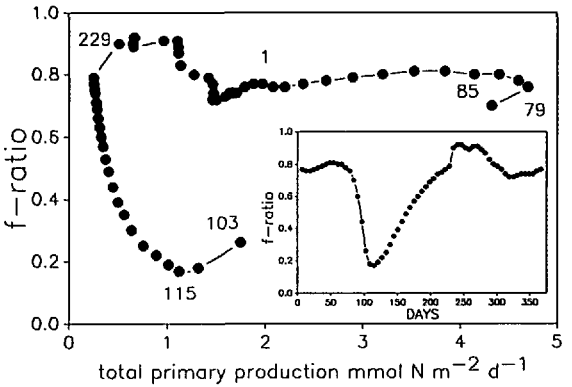

Figure 12. Annual cycles of *f*-ratio and net primary production, for 10 m/day run, plotted as a phase diagram to show annual trajectories and covariance as in Figure 11. Inset: annual cycle of *f*-ratio.

e. New production and the f-ratio. The fraction of the total production supported by new nitrate supplied from below the euphotic zone is called the *f*-ratio (Eppley and Peterson, 1979). Since regenerated production is also part of the total, variations in the *f*-ratio are regulated by the concentrations of NO_3 and NH_4 as specified by Eqs. 2, 3, 6, 19 and 20 in our model, and as suggested by Harrison *et al.* (1987). Three separate processes are important: the concentration-dependent uptake rates of NO_3 and NH_4, and the concentration-dependent inhibitory effect of NH_4 on NO_3 uptake (see above). Following Eppley and Peterson (1979) and Harrison *et al.* (1987), we plot *f* on total production and nitrate for the 10 m/day sinking rate scenarios in Figures 12 and 13. *f* varies annually from 0.2–0.9 (Fig. 12, inset), and reaches its minimum value only briefly because the high rate of detrital fallout removes the principal source of regeneration from the system and limits zooplankton and bacterial stocks in summer.

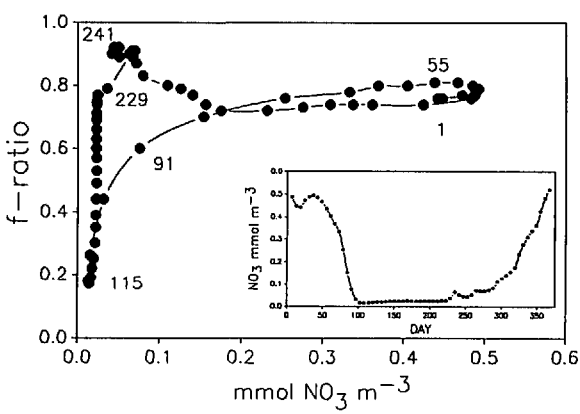

Figure 13. Annual cycles of *f*-ratio and nitrate, for 10 m/day run, plotted as in Figure 12. Inset: as Figure 5a.

Thus f increases as the heterotrophic stocks decline in summer, then continues to increase when nitrate input resumes after day 223, even though bacteria and zooplankton recover late in the year.

f is relatively constant as primary production rises, driven solely by nitrate input, between days 1–79 (Fig. 13), then declines as primary production falls after NO_3 inputs are limited to diffusion. f rises while production continues to fall between days 115–223, while NO_3 stays at low levels (Fig. 13 inset) because regenerated production is declining at that time. However, it should be remembered that as the model does not allow for nutrient trapping by the deep chlorophyll maximum, f-ratios are likely to be overestimated during the summer. Finally, f reaches its maximum value as NO_3 inputs increase in the fall, and production starts to rise again, ending the cycle and the year where it began. The cycle is similar in the 1 m/day run, except that f is low for a longer period in summer, and does not get quite as high in winter.

The f vs NPP plot resembles the plot of f vs. primary production for individual stations in the Southern California Bight (Eppley and Peterson, 1979). We suggest that one possible reason for the relationship presented by those investigators is that the annual cycles of f and NPP behave as our model suggests, driven by the annual cycle of nitrate input, as modulated by nitrogen regeneration. We caution however, that our results are valid for the mixed layer in a seasonal model only, and that considerable variation in the shapes of such curves may exist, even in other model runs, not to mention in the real world (cf. Sarmiento *et al.*, 1990).

f. Detailed zooplankton/bacterial/NH_4 dynamics of the 10 m/day run. The description of the gross behavior of the standing stocks just presented ignores a large amount of information which is provided in the model output. Some of the possibilities inherent in a full flow-oriented model are suggested below, in our analysis of the dynamics of some of the biogenic compartments. We limit our consideration to the behavior of the zooplankton, bacterial, and NH_4 stocks for the 10 m/day case.

In our model, there is just one zooplankton compartment which carries out all three modes of phagotrophic ingestion: herbivory, bacterivory and detritivory. Peak levels of inputs to and output from the zooplankton compartment occur during the maximum zooplankton biomass period between days 79–123 (Fig. 14a,c). In this model run, herbivory is always the greatest source of nutrition, contributing 75–100% of the zooplankton diet (Fig. 14b). In the 1 m/day runs, where detrital fallout is reduced the variation in dietary composition is more pronounced, and bacteria are equally important with phytoplankton as a source.

Sinks for zooplankton biomass include mass-specific rates of NH_4 and DON excretion, egestion and predation by unmodelled higher consumers. Egestion is a function of the ingestion rates, and predation has been expressed (Eq. 7) as a mass-specific rate as well. The relative importance of the four loss terms are largely determined by the parameter choices, and are quite constant throughout the year.

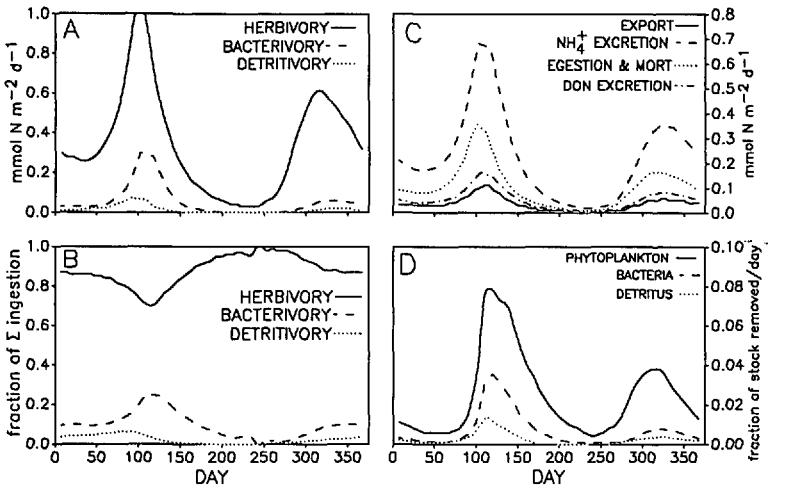

Figure 14. Zooplankton dynamics from 10 m/day run. Annual cycles of: (a) total ingestion and (b) proportional ingestion of each food type; (c) total losses and (d) clearance of bacterial and phytoplankton standing stocks.

Excretion is the principal removal term, accounting for about half the total losses. All the rates are thus closely coupled to biomass, and have peaks in spring and fall, corresponding to the utilization of the spring and fall blooms (Fig. 14c). Following the decline in phytoplankton and detrital stocks after the spring bloom, zooplankton ingestion and thus excretion are severely limited by food availability. Zooplankton production reaches a maximum of 0.3 mMol m^{-2} day^{-1} near day 100 and is negative (i.e., stock is declining) during the summer. The impact of zooplankton grazing can be seen in Figure 14d. Although at times over 75% of the daily primary and bacterial production are removed, only small fractions of the standing stocks are removed each day. These levels of removal are consistent with field observations (e.g., Ducklow *et al.*, 1989 and citations therein).

In this nitrogen flow model, bacteria are sustained solely on labile dissolved organic nitrogen (DON) and NH_4, and excrete only NH_4. There is no separate mortality term, but the mass-specific excretion rate may be considered to include mortality. In such a case, it is tacitly assumed that dead bacterial biomass is quickly converted to NH_4. A separate mass specific mortality term defining the flux of bacterial nitrogen to detritus could be included. Bacterial production, calculated as (NH_4 uptake + DON uptake − NH_4 excretion), ranges from 0 to 0.8 mmol m^{-2} day^{-1} (Fig. 15a), which is slightly less than the dynamic range for zooplankton herbivory and about twice the range for zooplankton production. Bacterial production is very slightly negative in late summer, when NH_4 excretion exceeds the combined uptake of NH_4 + DON. This is because the fluxes of DON and NH_4 are much reduced at this period of low stocks following removal of the biomass and detritus generated during the spring bloom. At

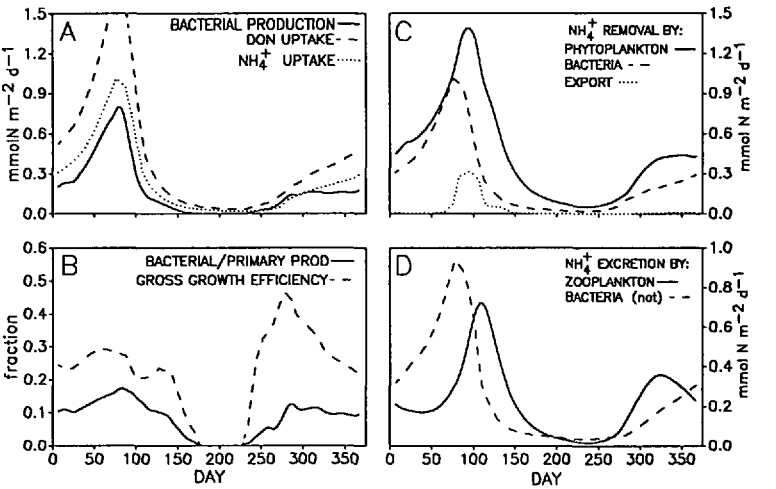

Figure 15. Bacterial and ammonium dynamics of 10 m/day run. Annual cycles of (a) bacterial production and uptake; (b) ratio of bacterial:primary production and gross growth efficiency; (c) NH_4 removal by bacteria and phytoplankton, and (d) NH_4 supply by bacteria and zooplankton.

this time the bacterial stock is still sufficiently high that the mass specific excretion rate constant produces an excess of excretion over uptake. Bacterial production is always positive in the 1 m/day run. In general, excretion is the largest loss term for the bacteria, just as it was for the zooplankton. Export is important briefly during the detrainment season, whereas bacterivory is never more than 30%, and usually less than 10% of the total losses. The importance of bacterivory may be greater in a model with two size classes of zooplankton.

Specific growth rates for bacteria (Production/biomass ratios) range from 0–0.04 per day (data not shown). This may seem low since rates in excess of 1/day have been reported (Azam *et al.*, 1983). However, gross growth efficiencies (production/total input) are in the range of typical values of 0.2–0.5 (Fig. 15b; cf. Bjornsen, 1986), except during the period when production declines to zero. We calibrated the bacterial excretion parameter to maintain the gross growth efficiencies in this range. Furthermore, except during the same period, bacterial production is 10–20% of primary production, not much lower than the range reported in the literature (Fig. 15b; cf. Cole *et al.*, 1988). Together these results suggest that growth rates are not low because uptake rates or production are unusually low. Rather, growth rates are low because the expected production rates yield low values when divided by high bacterial biomass levels. In this model run, bacterial stocks are always higher than zooplankton stocks and bacterivory is low, allowing bacterial stocks to stay high. Thus we have a scenario in which a large amount of nitrogen is tied up in bacterial biomass, which turns over

slowly. Kirchman (pers. comm.) has found support for this scenario in the subarctic North Pacific.

NH_4 utilization is by both bacteria and phytoplankton, with a peak around the time of the spring bloom (Fig. 15c). Bacteria compete effectively for NH_4 until the peak of the bloom, and during most of the fall and winter, with phytoplankton taking a major share only during the period during the bacterial decline after stratification. Over the course of the year, bacterial uptake is 37% of the total, in good agreement with the estimates of Wheeler and Kirchman (1986). NH_4 excretion (supply) rates are shown in Fig. 15d. We have plotted the net bacterial excretion (excretion minus bacterial uptake) to show the relative roles of bacteria vs zooplankton in supplying NH_4 for phytoplankton. Bacteria dominate as suppliers of NH_4 for phytoplankton until the peak of the bloom, when herbivory and detritivory increase and allow the zooplankton to take over as major sources of NH_4 in the midsummer. After heavy detrital fallout has removed most of the biomass generated in the bloom, NH_4 supply rates fall to very low values.

6. Discussion

a. The seasonal cycles. Our results bear on questions regarding the mechanisms responsible for the generation and maintenance of phytoplankton blooms in regions with seasonally varying mixed layers. In many of our previous model runs, we have observed annual cycles for phytoplankton biomass like the one produced in the present 10 m/day case (Figs. 5, 6), in which there is either no spring bloom, or one which differs little from subsequent blooms in the same year. As Evans and Parslow (1985) and Frost (1987) have also shown, interactions between the annual cycles of mixing and grazing regulate the timing and amplitude of the spring bloom. Menzel and Ryther's (1960) data (Fig. 5) show that there is considerable variability in these features. Clearly the release of the phytoplankton from nutrient and light limitation by restratification is not always a sufficient condition for a classic spring bloom. Our model provides a flexible tool for further exploration of the effects of foodweb structure and nutrient cycling on bloom dynamics.

The simulated seasonal cycles have demonstrated the great importance of the amplitude and duration of the spring bloom, and the subsequent removal of biomass generated by the bloom, in governing the dynamics of production and biomass during the annual cycle. Comparison of the 1 and 10 m/d^{-1} scenarios shows that when sinking rates are high and the spring biomass is rapidly lost from the system, summer production is limited because nutrient regeneration is limited to the cycling of living phytoplankton biomass. Detrital material behaves like a capacitor, allowing higher regeneration rates and greater production. When sinking rates are high, regeneration is low, and vice-versa. Clearly this result would be modulated by diffusion rates in summer. To some extent, the effects of detrital residence times on regeneration can be

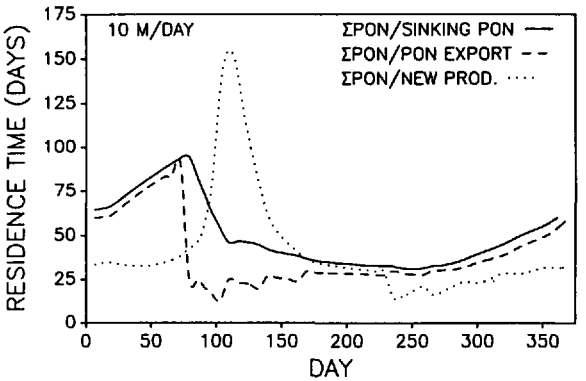

Figure 16. Residence times of total particulate nitrogen in the mixed layer.

offset by increasing diffusion of nitrate. This will enhance new production and keep higher levels of biogenic nitrogen in the system, allowing higher production and regeneration (Fig. 3). Our simplified model suggests that in temperate systems, the biogeochemical dynamics of the mixed layer may be dominated by the relative importance of the spring bloom, and removal and diffusion rates in summer.

The importance of the mean sinking rate in maintaining particulate nitrogen in the mixed layer is summarized in Figure 16, which shows the residence times of the total particulate organic nitrogen (phytoplankton + bacteria + zooplankton + detritus) in the mixed layer in our two runs. Instantaneous residence times (i.e., total PON/(new production or PON export)) range from ca 10 to over 100 days in the 10 m/d^{-1} case and from ca 1–600 days in the 1 m d^{-1} case. The estimate of residence time suggested by Eppley *et al.* (1983), PON/sinking flux, is also shown. Because sinking is not the only export term, this provides overestimates of the exact residence time, but the comparison is good for the 10 m d^{-1} results, in which sinking was more important than the 1 m d^{-1} case. Estimates and annual cycles of residence times depend strongly on whether they are calculated as pool size/input or pool size/output, because the system is not in steady state. Thus residence times calculated from new production rates (cf. Eppley *et al.*, 1983) are generally lower, but with a higher peak, than those estimated from export.

The simulated seasonal cycles of *f*-ratio, nitrate, and net primary production (NPP) result in a positive convex relationship between *f* and both NPP (the Eppley curve; Fig. 12) and nitrate (Fig. 13) that is consistent with observations (Eppley *et al.*, 1979; Eppley and Peterson, 1979; Harrison *et al.*, 1987). We suggest that these observations may be reflections of the trajectories of the plankton system in the *f*-NPP and *f*-NO_3 phase planes over the seasonal cycle. Furthermore, the *f*-NPP curve was simulated without having to assume a nonlinear relationship between detrital sinking flux and sinking rate as was found to be necessary using the model of Vezina and Platt (1987).

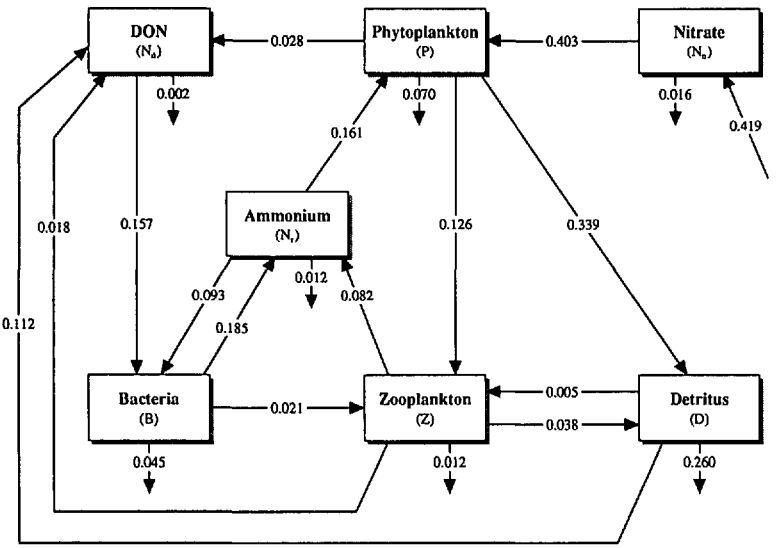

Figure 17. Modelled annual nitrogen fluxes for the 10 m/day run. Units are Mol N m^{-2} y^{-1}.

b. The annual budget. Annual fluxes in the marine ecosystem are difficult, if not impossible, to measure by any reasonable observational program and so the results from properly validated models may represent the only method of estimating them. Although the present model is highly simplified, we consider that some discussion of the simulated annual fluxes would be useful and will focus on the annual fluxes for the 10 m d^{-1} simulation (Fig. 17). The net annual upwards flux of nitrate is 0.40 Mol N m^{-2} y^{-1}, which is lower than, but not inconsistent with, Jenkins' (1988) estimate for the Bermuda region of 0.56 ± 0.16 Mol N m^{-2} y^{-1} determined from measurements of ^{3}He excess. Jenkins made the point that a nitrate flux of 0.6 Mol m^{-2} y^{-1} would imply an annual new production in excess of 3 Mol carbon m^{-1} (0.45 Mol N m^{-2} y^{-1}) for which there was other supporting evidence (Jenkins and Goldman, 1985). However, Jenkins was concerned that such a nitrate flux was greatly in excess of estimates of cross-thermocline diapycnal mixing, which he estimated as being of order 0.01–0.05 Mol N m^{-2} y^{-1} and Lewis *et al.* (1986) have estimated at 0.05 Mol m^{-2} y^{-1}. The results of our model have demonstrated that the largest contribution to nitrate import to the mixed layer is in fact entrainment and not diffusive mixing (Fig. 2b). For the 10 m d^{-1} simulation the diffusive flux was 0.07 Mol N m^{-1} y^{-1} (not very different from the estimates above) while the net entrainment flux was 0.34 Mol N m^{-2} y^{-1}. Thus entrainment accounts for 85% of the total flux and provides one possible way of explaining Jenkins' nitrate flux estimate.

It is also interesting to note that the model gives an annual new production of 0.40 Mol N m^{-2} y^{-1} which, using a Redfield ratio of 6.625, converts to a carbon new production of 2.67 Mol m^{-2} y^{-1}. This estimate is lower than either the Jenkins' (1988)

estimate of 3 Mol C m^{-2} y^{-1} discussed above or the estimate of 4.2 Mol C m^{-2} y^{-1} derived by Jenkins and Goldman (1985) from the long-term average of the seasonal oxygen cycle at Bermuda station "S". The latter estimate included the new production within the DCM, and so cannot be directly compared with our model estimate. In Section 4, it was shown that in 1959 the total production in the mixed layer was 73% of the total. If this same fraction is applied to the Jenkins and Goldman (1985) new production estimate a value of 3.1 Mol C m^{-2} y^{-1} is obtained, very close to the Jenkins (1988) value and close to the model estimate. Therefore, bearing in mind the different models and assumptions underlying these three estimates, the differences are not great. This supports the contention of Platt *et al.* (1989) that observations of the biogenic fluxes of oxygen and nitrogen can be reconciled with ^{14}C observations by appropriate models and averaging schemes, although as discussed next this implies very high *f*-ratios.

One surprising and slightly disturbing feature of the annual budget was the very high annual *f*-ratio of 0.71. This is much higher than the best available estimate of annual *f*-ratio for Bermuda Station "S", derived by Platt and Harrison (1985) from nitrate observations, which was 0.31. However, bearing in mind that our model was adjusted to give an ANPP of 3.7 Mol C m^{-2} y^{-1} approriate for Bermuda Station "S" (see Section 4), then a high *f*-ratio is a necessary consequence of achieving a new production close to the 3 Mol C m^{-2} y^{-1} suggested by the observations. It should be remembered that our estimate of mixed layer total ANPP was obtained from ^{14}C observations made in 1959, while the helium excess observations of Jenkins (1988) were made between 1985–86. If it was the case that the total ANPP was greater in 1985–86 than in 1959, then it would be possible to achieve a modelled new production of the right magnitude with a lower annual *f*-ratio. Smith *et al.* (1987) reported a total primary production for the full euphotic zone of ca 90 gC m^{-2} y^{-1} for Station S. This value in combination with the Jenkins (1988) and Jenkins and Goldman (1985) estimates of new production, implies annual *f*-ratios of 0.4–0.56. A simulation using a submixed layer nitrate concentration of 2.25 mMol N m^{-3}, a phytoplankton mortality of 0.015 d^{-1} would give a new production of 2.9 Mol C m^{-2} y^{-1}, a total production of 5.9 Mol C m^{-2} y^{-1} and an *f*-ratio of 0.49 (Fig. 3). Alternatively, one could accept the observed value for total production and produce a model with a lower new production and *f*-ratio. At the moment it is impossible to decide between these two options because of the absence of reasonably complete seasonal data for new and regenerated production for the Bermuda area or any other oligotrophic oceanic site in the North Atlantic.

We have discussed the model annual fluxes that can be compared with observations from Station "S" and have found that model and data are in good general agreement. It is therefore of interest to look at some of the other annual flux estimates for which there are not observational data. There has been much debate about the relative importance of zooplankton and bacteria in the regeneration of ammonium (Harrison, 1980; Ducklow, 1983; King, 1987). The seasonal cycle of modelled ammonium

regeneration (Fig. 15d) showed that in winter and early spring bacteria were the larger source of regeneration, with zooplankton taking this role throughout the remainder of the year. Averaged over the whole year the net bacterial regeneration was just 12% larger than the zooplankton regeneration for the 10 m d^{-1} detrital sinking rate (Fig. 17), while for the 1 m d^{-1} sinking rate it was 76% larger. The difference between the two simulations reflects the greater recycling of detritus for lower sinking rates and the overriding importance of detrital breakdown for the modelled supply of DON to the bacteria. We know of no annual data with which to compare these estimates.

The model described in this paper should be regarded as a first attempt to elucidate the important factors involved in the recycling of nitrogen in the euphotic zone. There have been previous models that have incorporated nitrogen recycling (Jamart *et al.*, 1977; Kiefer and Kremer, 1981; King, 1987), but, apart from the model of Vezina and Platt (1986), none of these have attempted explicitly to model the role of both zooplankton and bacteria. Even so the ecological structure of the present model is still highly aggregated; it is highly probable that future models will incorporate different size classes of organisms and be multi-element in their structure (Lancelot and Billen, 1986). The physical structure of the model is also highly simplified and does not include such processes as diel changes in turbulent mixing (Woods and Onken, 1982), the effect of internal waves (Joyce, 1988), and seasonal changes in the diffusive mixing across the thermocline and within the mixed layer, let alone the effects of horizontal advection. Furthermore, the summer deep chlorophyll maximum, which can have a major effect on the flux of nitrate into the mixed layer (Herbland and Voiturez, 1979; Fasham *et al.*, 1985), is not included in the model. The effect of some of these processes on the nitrogen cycle will be discussed in a companion paper which describes the results of embedding the ecological model described in this paper into a 3-D General Circulation Model of the North Atlantic (Sarmiento *et al.*, 1990).

Acknowledgments. This research was supported by grants from Natural Environmental Research Council and U. S. Dept of Energy (DOE Subcontract No. 19X-SC167V.) to M.J.R.F., and by NSF grant OCE8904229 to H.W.D. We thank J. Sarmiento, R. Toggweiler, G. Evans, T. Platt and J. Wroblewski for discussions or for reading early drafts.

APPENDIX A

The zooplankton feeding formula

The overall effect of total food levels on zooplankton grazing was parameterized using a Michaelis-Menten equation. A measure of total food, F, can be defined as,

$$F = p_1P + p_2B + p_3D \tag{A1}$$

where p_1, p_2, p_3 are measures of the zooplankton preferences for the various food types. The grazing rate on phytoplankton can then be defined as,

$$G_1 = gZ\frac{p_1P}{K_3F}$$

where g is the maximum specific grazing rate, and K_3 is the half-saturation constant for grazing.

The relationship between total grazing and the concentration of the various food items will depend on the precise formulation chosen for the preferences. The simplest formulation would be to assign constant values (e.g. Evans, 1988) proportional to the assumed feeding preference of the zooplankton. There are, however, certain disadvantages with this method. Firstly, preliminary trials with the model showed that the results were very sensitive to the choice of such constant preference values. As there are very few quantitative data on zooplankton food preference values, or their seasonal variability, this is a matter of some concern. Furthermore, the model zooplankton graze on phytoplankton, bacteria and detritus and are therefore a highly aggregated entity incorporating organisms from flagellates to euphausiids. It is therefore difficult, in principle, to assign constant preferences as the mix of zooplankton organisms, and therefore the preferences, will change throughout the year depending on the available food. Such considerations suggests that the assigned preferences should in some way change dynamically as a function of the relative proportion of the food. In general such a system could be achieved by defining weighted preferences, p_i', thus,

$$p_i' = \frac{p_i f(X_i)}{\sum_j p_j f(X_j)} \tag{A2}$$

where $f(X_i)$ is some function of X_i and the summation is over all the different food types. The simplest functional expression for f is to choose $f(X_i) = X_i$ (Hutson, 1984). Thus the preference for phytoplankton would be,

$$p_i' = \frac{p_1 P}{(p_1 P + p_2 B + p_3 D)} \tag{A3}$$

where the p_1, p_2, p_3 are the assumed nominal preferences for phytoplankton, bacteria and detritus when the concentrations of these foods are equal. This is equivalent to assuming that the zooplankton actively select the most abundant food organism, or, as we are dealing with an aggregated entity, that particular subgroups of zooplankton will develop to crop the most abundant organisms. Another form for $f(X_i)$ was suggested by Pace *et al.* (1984), who assumed that the $f(X_i)$ were equal to the normalized limitation functions describing the zooplankton ingestion of the ith food type; the resulting preferences would obviously depend on the particular functional form assumed for the limitation function, and the choice of parameters for that function.

The effect of these various possibilities can be visualized for the case of two food resources by calculating the total zooplankton grazing rate, $G_t = G_1 + G_2$, as a function of the food concentrations X_1 and X_2 using the three different preference formulations. Eq. A2 (with $Z = g = 1$ and $K_3 = 1$) was used to define the ingestion rates for the two resources and a value of 0.5 was assumed for p_1 and p_2.

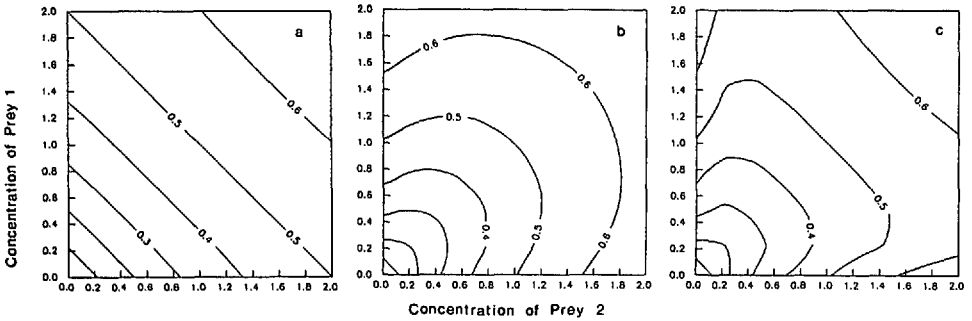

Figure 18. Contours of theoretical predator total grazing rate as a function of the concentration of two prey resources for (a) constant preferences, (b) variable preferences proportional to the prey concentrations, (c) variable preferences proportional to the predator's potential grazing pressure on the prey. See text for details.

The contours of total grazing (Fig. 18) show that the three formulations give identical results when $X_1 = X_2$, but differ when either X_1 or X_2 approach zero. For example when $X_1 = 0$ then, for the Evans case, X_2 must equal 2 before the total grazing rate equals 0.5. However, in both the other cases the grazing rate equals 0.5 for $X_2 = 1.0$. In the case of the Hutson expression, the contours show that the switching occurs uniformly as X_2 becomes less than X_1, whereas for the Pace expression the switching only occurs markedly when $X_2 < X_1/2$. Another consequence of the nonlinearity of the Hutson and Pace switching is that as X_1 or X_2 approach zero the total grazing G_t can actually increase. This behavior might be rationalized by assuming that zooplankton use up energy in having to switch between different prey types. We know of no data that might lend support to any of these switching functions and so it might be argued that the simplest model, i.e. the constant preferences, should therefore be adopted. However, preliminary simulations showed that using the Hutson expression increased the likelihood of a zooplankton population surviving the winter, thereby producing a more robust model. Accordingly, the Hutson switching function was adopted, although we feel that the parameterization of zooplankton feeding preferences is a topic requiring further theoretical development.

The final chosen form for the grazing of zooplankton on phytoplankton can be obtained by substituting the Hutson formula for the p_i' values for the p_i values in Eqs. A1 and A2 to give,

$$G_1 = \frac{gZp_1P^2}{K_3(p_1P + p_2B + p_3D) + p_1P^2 + p_2B^2 + p_3D^2}. \qquad \text{(A4)}$$

When B or D are zero or constant fractions of P then this expression will reduce to the standard Michaelis-Menten equation.

APPENDIX B

Parameter sensitivity analysis

Parameter sensitivity analysis of models with even a modest number of parameters presents considerable problems as it is computationally prohibitive to consider varying the parameters independently across the whole of the possible parameter space. There are various solutions to this problem (Kremer, 1983) but the procedure we adopted was to test the sensitivity of each parameter in turn by running a standard case with the given parameter altered, first to a higher and then a lower value. The choice of upper and lower values was based, where possible, on a knowledge of the likely range of the parameter in question. If such information was not available the low and high values were chosen to be half and twice the standard value respectively (see Table 2 for choice of values). For each parameter choice the model was run to a steady-state and various statistics of the annual cycle were calculated, such as the mean, standard deviation, and highest and lowest value for each variable, the total annual net primary production (ANPP), and the annually averaged *f*-ratio (total annual new production divided by ANPP). The effect of a given parameter, p, was quantified by calculating a normalized sensitivity, $S(p)$, defined as,

$$S(p) = \left(\frac{(E(p) - E_s)}{E_s}\right) \Big/ \left(\frac{(p - p_s)}{p_s}\right) \tag{B1}$$

where E_s is the value of a given statistic for the standard case with parameter value p_s, and $E(p)$ is the value for the case when the parameter is given the value p. This index measures the fractional change in the statistic for a fractional change in the parameter. As an example, we have calculated the values of S for ANPP and the annually averaged *f*-ratio. The results (Table 2) give an estimate of how much ANPP or the *f*-ratio will be altered by a different value of each parameter.

The first point of interest arising from this study was that the value of $S(p)$ for an increased value of a parameter was similar in magnitude to that for a decreased value; if this had not been the case then it would have suggested that the standard run of the model was close to some discontinuity in the response surface of the model.

The second point to note was that the $S(p)$ values for ANPP were of the same order, but of opposite sign, to those for the *f*-ratio. The reason for this can be seen by plotting the *f*-ratio values against the ANPP values for all the sensitivity runs (Fig. 19), which shows that the two variables are highly negatively correlated ($R^2 = 80\%$). This is at first sight a surprising result which apparently runs counter to the presently accepted paradigm of the relationship of *f*-ratio to total primary production (Eppley and Peterson, 1979), which postulates a positive parabolic functional relationship between the two variables (the Eppley curve). However, it should be remembered that the data which was used by Eppley and Peterson was based on experiments lasting only a few hours, whereas the simulated data shown in Figure 19a are averages over one year of

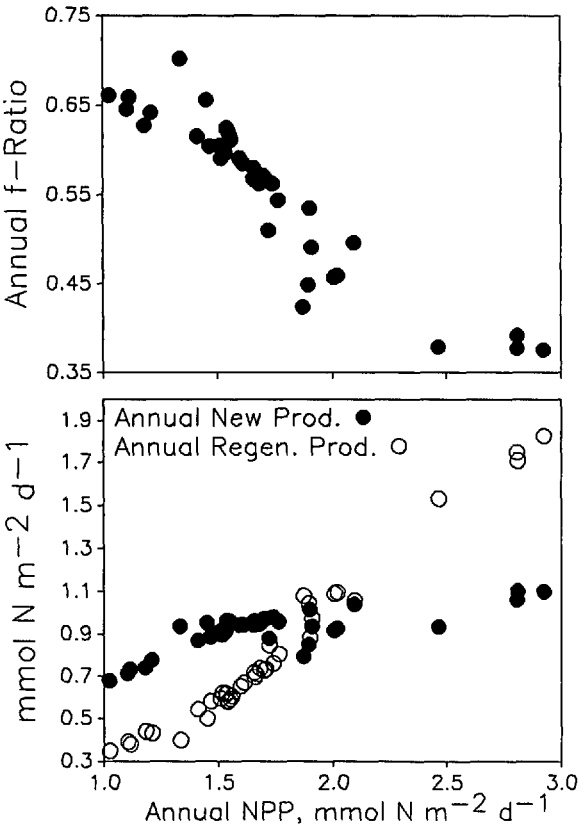

Figure 19. (a) Annual *f*-ratio vs Annual Net Primary Production (ANPP) for all sensitivity runs. Each point is the annual *f* and ANPP for a given run. (b) Annual new and regenerated production vs. ANPP for the same runs.

model time; there is no reason to expect the relationships for these very different averaging periods to be the same.

The negative correlation between *f* and ANPP can be explained most simply if we consider the subset of the sensitivity runs that involved only food web parameters, that is excluding the parameters associated with physical forcing factors such as light and nutrient diffusion. In Figure 19b the annual total new and regenerated production for this subset has been plotted against ANPP. This graph shows that between ANPP values of 1.3–2.5 the new production hardly changes, while regenerated production increases by a factor of 5 thus giving rise to the negative relationship between *f* and ANPP. This result shows that changing food web parameters can have a large effect on regenerated production, but only a second order effect on new production, which is controlled mainly by factors such as mixed layer depth, diffusion rate, and deep nitrate concentration (see further discussion of these points in Section 4).

The parameter sensitivities can be divided into three classes (Table 2). There are those that do not have a large effect on the value of NPP or the *f*-ratio, such as cloudiness, light attenuation coefficient due to phytoplankton, phytoplankton exudation fraction, zooplankton excretion rate, diffusion mixing rate, and all the bacterial parameters. Then there are the parameters that have a large effect, such as the light attenuation due to water, the PAR: total irradiance ratio, the initial slope of the P-I curve, phytoplankton mortality rate and half-saturation parameter, and the deep nitrate concentration. Finally, there are parameters whose effect is intermediate such as phytoplankton maximum uptake rate, zooplankton mortality rates and assimilation efficiency, zooplankton half-saturation constant, detrital breakdown and sinking rates, and nitrate inhibition parameter.

Some caution should be exercised in using these results; they only apply to the particular run of the model that was used as the standard case, and they cannot reveal any critical effects that might be due to interactions between sets of parameters. However, they do at least give an initial idea of where research might be directed to improve the predictive power of the model.

REFERENCES

Altabet, M. A. 1989. Particulate new nitrogen fluxes in the Sargasso Sea. J. Geophys. Res., *94,* 12771–12779.

Azam, F., T. Fenchel, J. G. Field, J. S. Gray, L. A. Meyer-Reil and F. Thingstad. 1983. The ecological role of water-column microbes in the sea. Mar. Ecol. Prog. Ser., *10,* 257–263.

Baker, K. S., and R. Frouin. 1987. Relation between photosynthetically available radiation and total insolation at the ocean surface under clear skies. Limnol. Oceanogr., *32,* 1370–1377.

Bannister, T. T. 1974. A general theory of steady state phytoplankton growth in a nutrient saturated mixed layer. Limnol. Oceanogr., *19,* 13–30.

Be, A. W. H., J. M. Forns and O. A. Roels. 1971. Plankton abundance in the North Atlantic Ocean, *in* Fertility of the Sea, Vol. 1, J. D. Costlow, ed., Gordon and Breach Science Publishers, 17–50.

Beers, J. F., F. M. H. Reid and G. I. Stewart. 1982. Seasonal abundance of the microplankton population in the North Pacific Gyre. Deep-Sea Res., *29,* 227–246.

Bermuda Biological Station. 1960. The plankton ecology, related chemistry and hydrography of the Sargasso Sea, Final report, part 3, US AEC Contract AT(30-1)-2078.

Bjornsen, P. K. 1986. Bacterioplankton growth yield in continuous seawater cultures. Mar. Ecol. Prog. Ser., *30,* 191–196.

Brock, T. D. 1981. Calculating solar radiation for ecological studies. Ecol. Modell., *14,* 1–19.

Brzezinski, M. A. 1987. Colorimetric determination of nanomolar concentrations of NH_4^+ in seawater using solvent extraction. Mar. Chem., *20,* 277–288.

—— 1988. Vertical distribution of ammonium in stratified waters. Limnol. Oceanogr., *33,* 1176–1182.

Carlucci, A. F., D. B. Craven and S. M. Heinrichs. 1985. Diel production and microheterotrophic utilization of dissolved free amino acids in waters off Southern California. Appl. Environ. Microbiol., *48,* 165–170.

Clarke, K. R. and I. R. Joint. 1986. Methodology for estimating numbers of free-living and attached bacteria in estuarine water. Appl. Env. Microbiol., *51,* 1110–1120.

Cole, J. J., M. L. Pace and S. Findlay. 1988. Bacterial production in fresh and saltwater ecosystems: a cross-system overview. Mar. Ecol. Prog. Ser., *43,* 1–10.

Conover, R. J. 1978. Transformation of organic matter, *in* Marine Ecology, Vol. 4, O. Kinne, ed., Wiley, 221–500.

Corner, E. D. S. and B. S. Newell. 1967. On the nutrition and metabolism of zooplankton. IV. The forms of nitrogen excreted by *Calanus*. J. Mar. Biol. Assoc. U.K., *47,* 113–120.

Davis, C. S. 1987. Components of the zooplankton production cycle in the temperate ocean. J. Mar. Res., *45,* 947–983.

Deevey, G. 1971. The annual cycle in quantity and composition of the zooplankton of the Sargasso Sea of Bermuda. I. The upper 500 m. Limnol. Oceanogr., *16,* 219–240.

Ducklow, H. W. 1983. Production and fate of bacteria in the ocean. Bioscience, *33,* 494–501.

Ducklow, H. W., M. J. R. Fasham and A. F. Vezina. 1989. Flow analysis of open sea plankton networks, *in* Network Analysis in Marine Ecology, F. Wulff, J. G. Field and K. H. Mann, eds., Coastal and Estuarine Studies, Vol. 32, Springer-Verlag, 159–205.

Ducklow, H. W. and S. M. Hill. 1985. Tritiated thymidine incorporation and the growth of heterotrophic bacteria in warm core rings. Limnol. Oceanogr., *30,* 260–272.

Dugdale, R. C. and J. J. Goering. 1967. Uptake of new and regenerated forms of nitrogen in primary production. Limnol. Oceanogr., *12,* 196–206.

Eppley, R. W. 1972. Temperature and phytoplankton growth in the sea. Fish. Bull., *70,* 1063–1085.

Eppley, R. W. and B. J. Peterson. 1979. Particulate organic matter flux and planktonic new production in the deep ocean. Nature, *282,* 677–680.

Eppley, R. W., E. H. Renger and P. R. Betzer. 1983. The residence time of particulate organic carbon in the surface layer of the ocean. Deep-Sea Res., *30,* 311–323.

Eppley, R. W., E. H. Renger and W. G. Harrison. 1979. Nitrate and phytoplankton production in Southern California coastal waters. Limnol. Oceanogr., *24,* 483–494.

Esaias, W. E., G. C. Feldman, C. R. McClain and J. A. Elrod. 1986. Monthly satellite-derived phytoplankton pigment distribution for the North Atlantic Ocean basin. EOS, 835–837.

Evans, G. T. 1988. A framework for discussing seasonal succession and coexistence of phytoplankton species. Limnol. Oceanogr., *33,* 1037–1036.

Evans, G. T. and J. S. Parslow. 1985. A model of annual plankton cycles. Biol. Oceanogr., *3,* 327–347.

Fasham, M. J. R. 1985. Flow analysis of materials in the marine euphotic zone, *in* Ecosystem Theory for Biological Oceanography, R. E. Ulanowicz and T. Platt, eds., Can. Bull. Fish. Aquat. Sci., *213,* 139–162.

Fasham, M. J. R., P. M. Holligan and P. R. Pugh. 1983. The spatial and temporal development of the spring phytoplankton bloom in the Celtic Sea, April 1979. Prog. Oceanogr., *12,* 87–145.

Fasham, M. J. R., T. Platt, B. Irwin and K. Jones. 1985. Factors affecting the spatial pattern of the deep chlorophyll maximum in the region of the Azores front. Progr. Oceanogr., *14,* 129–165.

Fenchel, T. and T. H. Blackburn. 1979. Bacteria and Mineral Cycling. Academic Press, New York, 225 pp.

Fogg, G. E. 1983. The ecological significance of extracellular products of phytoplankton photosynthesis. Botanica Marina, *26,* 3–14.

Frost, B. W. 1987. Grazing control of phytoplankton stock in the open subarctic Pacific Ocean: a model assessing the role of mesozooplankton, particularly the large calanoid copepods *Neocalanus* spp. Mar. Ecol. Prog. Ser., *39,* 49–68.

Fuhrman, J. A. 1987. Close coupling between release and uptake of dissolved free amino acids in seawater studied by an isotope dilution approach. Mar. Ecol. Prog. Ser., *37,* 45–52.

Glibert, P. M., D. C. Biggs and J. J. McCarthy. 1982. Utilization of ammonium and nitrate during austral summer in the Scotia Sea. Deep-Sea Res., *29,* 837–850.

Goldman, J. C., D. A. Caron and M. R. Dennett. 1987. Regulation of gross growth efficiency and ammonium regeneration in bacteria by substrate C:N ratio. Limnol. Oceanogr., *32,* 1239–1252.

Goldman, J. C. and P. M. Glibert. 1983. Kinetics of inorganic nitrogen uptake by phytoplankton, *in* Nitrogen in the Marine Environment, E. J. Carpenter and D. G. Capone, eds., Academic Press, 233–274.

Harrison, W. G. 1980. Nutrient regeneration and primary production in the sea, *in* Primary Productivity in the Sea, P. G. Falkowski, ed., Plenum, 433–460.

Harrison, W. G., T. Platt and M. R. Lewis. 1987. *F*-ratio and its relationship to ambient nitrate concentration in coastal waters. J. Plank. Res., *9,* 235–248.

Herbland, A. and B. Voituriez. 1979. Hydrological structure analysis for estimating the primary production in the tropical Atlantic Ocean. J. Mar. Res., *37,* 87–101.

Hutson, V. 1984. Predator mediated coexistence with a switching predator. Math. Biosci., *68,* 233–246.

Isemer, H. J. and L. Hasse. 1985. The Bunker climate atlas of the North Atlantic Ocean, Vol. 1: Observations, Springer-Verlag.

Jamart, B. M., D. F. Winter, K. Banse, G. C. Anderson and R. K. Lam. 1977. A theoretical study of phytoplankton growth and nutrient distribution in the Pacific Ocean of the northwestern U. S. coast. Deep-Sea Res., *24,* 753–773.

Jenkins, W. J. 1988. Nitrate flux into the euphotic zone near Bermuda. Nature, *331,* 521–523.

Jenkins, W. J. and J. C. Goldman. 1985. Seasonal oxygen cycling and primary production in the Sargasso Sea. J. Mar. Res., *43,* 465–491.

Jerlov, N. G. 1976. Marine Optics, Elsevier.

Jitts, H. R., A. Morel and Y. Saijo. 1976. The relation of oceanic primary production to available photosynthetic irradiance. Aust. J. Mar. Fresh. Res., *27,* 441–454.

Johannes, R. E. and K. L. Webb. 1965. Release of dissolved amino acids by marine zooplankton. Science, *146,* 923–924.

Jones, R. and E. W. Henderson. 1986. The dynamics of nutrient regeneration and simulation studies of the nutrient cycle. J. Conseil, *43,* 216–236.

Joyce, T. M. 1988. On the regulation of primary production by physical processes in the ocean: two case studies, *in* Toward a Theory of Biological-Physical Interactions in the World Ocean, B. J. Rothschild, ed., Kluwer, 39–51.

Kiefer, D. A. and C. A. Atkinson. 1984. Cycling of nitrogen by plankton: a hypothetical description based upon efficiency of energy conversion. J. Mar. Res., *42,* 655–676.

Kiefer, D. A. and J. N. Kremer. 1981. Origins of vertical patterns of phytoplankton and nutrients in the temperate, open ocean: a stratigraphic hypothesis. Deep-Sea Res., *28,* 1087–1106.

King, F. D. 1987. Nitrogen recycling efficiency in steady-state oceanic environments. Deep-Sea Res., *34,* 843–856.

Kremer, J. N. 1983. Ecological implications of parameter uncertainty in stochastic simulation. Ecol. Model., *18,* 187–207.

Lancelot, C. and G. Billen. 1986. Carbon-nitrogen relationships in nutrient metabolism of coastal marine ecosystems. Adv. Aquatic Micro-Biol., *3,* 263–321.

Lee, S. and J. A. Fuhrman. 1988. Relationships between biovolume and biomass of naturally-derived marine bacterioplankton. Appl. Environ. Microbiol., *52,* 1298–1303.

Levitus, S. 1982. Climatological atlas of the world ocean, NOAA Professional Paper 13, U. S. Govt. Printing Office.

Lewis, M. R., W. G. Harrison, N. S. Oakey, D. Herbert and T. Platt. 1986. Vertical nitrate fluxes in the oligotrophic ocean. Science, *234,* 870–873.

Lorenzen, C. J. 1972. Extinction of light in the ocean by phytoplankton. J. Cons., *34,* 262–267.

Menzel, D. W. and J. H. Ryther. 1960. The annual cycle of primary production in the Sargasso Sea off Bermuda. Deep-Sea Res., *6,* 351–367.

—— 1961. Zooplankton in the Sargasso Sea off Bermuda and its relation to organic production. J. Cons., *26,* 250–258.

Moloney, C. L., M. O. Bergh, J. G. Field and R. C. Newell. 1986. The effect of sedimentation and microbial regeneration in a plankton community: a simulation investigation. J. Plank. Res., *8,* 427–445.

Murray, J. W., J. N. Downs, S. Strom, C.-L. Wei, and H. W. Jannasch. 1989. Nutrient assimilation, export production and ^{234}Th scavenging in the eastern equatorial Pacific. Deep-Sea Res., *36,* 1471–1489.

Nelson, D. M., J. J. McCarthy, T. M. Joyce and H. W. Ducklow. 1989. Enhanced near-surface nutrient availability and new production resulting from the frictional decay of a Gulf Stream warm-core ring. Deep-Sea Res., *36,* 705–714.

Newell, R. C. and E. A. S. Linley. 1984. Significance of microheterotrophs in the decomposition of phytoplankton: estimation of carbon and nitrogen flow based on the biomass of plankton communities. Mar. Ecol. Prog. Ser., *16,* 105–119.

Pace, M. L., J. E. Glasser and L. R. Pomeroy. 1984. A simulation analysis of continental shelf food webs. Mar. Biol., *82,* 47–63.

Pace, M. L., G. A. Knauer, D. M. Karl and J. H. Martin. 1987. Particulate matter fluxes in the ocean: a predictive model. Nature, *325,* 803–804.

Paffenhofer, G-A. and S. C. Knowles. 1979. Ecological implications of fecal pellet size, production and consumption by copepods. J. Mar. Res., *37,* 35–49.

Parsons, T. P. and T. A. Kessler. 1987. An ecosystem model for the assessment of plankton production in relation to the survival of young fish. J. Plank. Res., *9,* 125–137.

Platt, T. and W. G. Harrison. 1985. Biogenic fluxes of carbon and oxygen in the ocean. Nature, *318,* 55–58.

Platt, T., W. G. Harrison, M. R. Lewis, W. K. W. Li, S. Sathyendranath, R. E. Smith and A. F. Vezina. 1989. Biological production in the oceans: the case for consensus. Mar. Ecol. Prog. Ser., *52,* 77–88.

Platt, T., K. H. Mann and R. E. Ulanowicz. 1981. Mathematical models in biological oceanography, UNESCO Press.

Poulet, S. A. 1983. Factors controlling utilization of nonalgal diets by particle-grazing copepods: a review. Oceanologica Acta, *6,* 221–234.

Riley, G. A. 1947. A theoretical analysis of the zooplankton population of Georges Bank. J. Mar. Res., *6,* 104–113.

Robinson, M. K., R. A. Bauer and E. Schroeder. 1979. Atlas of North Atlantic-Indian ocean monthly mean temperatures and mean salinities of the surface layer. U. S. Naval Oceanographic Office Reference Publication, 18.

Roy, S., R. P. Harris and S. A. Poulet. 1989. Inefficient feeding by *Calanus helgolandicus* and *Temora longicornis* on *Coscinodiscus wailesii:* quantitative estimation using chlorophyll-type pigments and effects on dissolved free amino acids. Mar. Ecol. Prog. Ser., *52,* 145–153.

Sarmiento, J. L., M. J. R. Fasham, R. Slater, J. R. Toggweiler and H. W. Ducklow. 1990. The role of biology in the chemistry of CO_2 on the ocean, *in* Chemistry of the Greenhouse Effect, M. Farrell, ed., Lewis Publ. (in press).

Schell, D. M. 1974. Uptake and regeneration of free amino acids in marine waters of Southeast Alaska. Limnol. Oceanogr., *19,* 271–278.

Sharp, J. H. 1977. Excretion of organic matter: do healthy cells do it? Limnol. Oceanogr., *22,* 381–399.

Smith, R. C. and K. S. Baker. 1981. Optical properties of the clearest natural waters. Appl. Opt., *20,* 177–184.

Smith, S. D. and F. W. Dobson. 1984. The heat budget at Ocean Weather Ship Bravo. Atmos.-Ocean., *22,* 1–22.

Smith, S. E. 1936. Environmental control of photosynthesis. Proc. Nat. Acad. Sci. USA *22,* 504–511.

Smith, S. L., W. O. Smith, L. A. Codispoti and D. L. Wilson. 1985. Biological observations in the marginal ice zone of the East Greenland Sea. J. Mar. Res., *43,* 693–717.

Smith, S. R., T. D. Jickells and A. H. Knap. 1987. Primary production in the Sargasso Sea: concurrent oxygen and carbon fluxes and an estimate of new production. Unpublished manuscript.

Steele, J. H. 1958. Plant production in the northern North Sea, Scottish Home Department, Marine Research Report No. 7. HMSO, Edinburgh.

Sugimura, Y. and Y. Suzuki. 1988. A high-temperature catalytic oxidation method of non-volatile dissolved organic carbon in seawater by direct injection of liquid samples. Mar. Chem., *14,* 105–131.

Suzuki, Y., T. Sugimura and T. Itoh. 1985. A catalytic oxidation method for the determination of total nitrogen dissolved in sea water. Mar. Chem., *16,* 83–97.

Toggweiler, J. R. 1989. Is the downward dissolved organic matter (DOM) flux important in carbon transport? *in* Productivity of the Oceans: Present and Past, W. H. Berger, V. S. Smetacek and G. Wefer, eds., Wiley, 65–83.

Toggweiler, J. R., J. L. Sarmiento, R. Najjar and D. Papademetriou. 1987. Models of chemical cycling in the oceans: a progress report. Ocean Tracers Laboratory Technical Report No. 4, Princeton University.

Verity, P. G. 1985. Ammonia excretion rates of oceanic copepods and implications for estimates of primary production in the Sargasso Sea. Biol. Oceanogr., *3,* 249–283.

Vezina, A. F. and T. Platt. 1986. Small-scale variability of new production and particulate fluxes in the ocean. Can. J. Fish. Aquat. Sci., *44,* 198–205.

Wallach, D. and B. Goffinet. 1989. Mean squared error of prediction as a criterion for evaluating and comparing system models. Ecol. Model., *44,* 299–306.

Walsh, J. J. 1983. Death in the Sea: Enigmatic phytoplankton losses. Prog. Oceanogr. *12,* 1–86.

Walsh, J. J. and R. C. Dugdale. 1972. Nutrient submodels and simulation models of phytoplankton production in the sea, *in* Nutrients in Natural Waters, J. Kramer and H. Allen, Wiley, 171–191.

Wheeler, P. A. and D. L. Kirchman. 1986. Utilization of inorganic and organic nitrogen by bacteria in marine systems. Limnol. Oceanogr., *31,* 998–1009.

Wiegert, R. G. 1979. Population models: experimental tools for the analysis of ecosystems, *in* Proceedings of Colloquium on Analysis of Ecosystems, D. J. Horn, R. Mitchell and G. R. Stairs, eds., Ohio State University Press, 239–275.

Williams, P. J. leB. 1981. Incorporation of microheterotrophic processes into the classical paradigm of the planktonic food web. Kieler Meeresforsch., *5,* 1–28.

Williams, P. M. and E. R. M. Druffel. 1988. Dissolved organic matter in the ocean: comments on a controversy. Oceanography, *1*, 14–17.

Woods, J. D. and R. Onken. 1982. Diurnal variation and primary production in the ocean—preliminary results of a Lagrangian ensemble model. J. Plank. Res., *4*, 735–756.

Wroblewski, J. 1977. A model of phytoplankton plume formation during variable Oregon upwelling. J. Mar. Res., *35*, 357–394.

Wroblewski, J. C., J. C. Sarmiento and G. R. Flierl. 1988. An ocean basin scale model of plankton dynamics in the North Atlantic. I. Solutions for the climatological oceanographic conditions in May. Global Biogeochem. Cycles, *2*, 199–218.

Received: *30, January 1990;* revised: *12 July, 1990.*